5

Laser Processing for Microengineering Applications

J. Brannon,* J. Greer,† and H. Helvajian‡

5.1 Introduction

Laser material processing is a technique by which materials can be fashioned in a nonintrusive manner with overall precision approaching the wavelength of the laser light. This processing is accomplished by exploiting the unique optical properties of the light to selectively remove or deposit material in a controllable manner. Materials thus processed to date include metals, ceramics, polymers, and semiconductors.

Microengineering is a discipline dealing with the design, materials synthesis, micromachining, assembly, integration, and packaging of miniature two-dimensional (2D) and three-dimensional (3D) sensors, microelectronics, and microelectromechanical systems (MEMS).[1] The physical structures and components have nominal dimensions, from the nanoscale to the microscale, and up to the millimeter scale. Microengineering has received worldwide attention because it promises to enable "intelligent" microinstruments with wide-ranging applications to be used in medicine, transportation, communications, and housing. Implicit in microengineering technology is the need to process materials with high dimensional accuracy, to process selective areas of the materials without incurring collateral damage to adjoining areas, and to prototype designs quickly without resorting to large-scale foundry operations. Laser material processing is uniquely qualified for microengineering because it can process materials without adhering to surface and crystallographic planes and can create millimeter-to-micron-scale structures in a broad range of materials. In addition, laser processing offers a number of capabilities that are complementary to both traditional material processing and semiconductor processing approaches. For example, lasers can process a large variety of materials, they can operate over large areas (meters squared) while maintaining high precision (less than microns), they can fashion materials by either selective removal or deposition, and they can alter materials through nonequilibrium chemical processes. These capabilities have profound consequences for both aeronautical and space applications, where specially "engineered" materials are often required and microengineering components using these novel materials may be necessary.

It is predicted that microengineering concepts will play an important role in the development of future aerospace systems. This prediction has bearing because the concepts make intelligent use of available volume and mass, and because microengineered components inherently use little energy. In more advanced applications, microengineering technology will enable the incorporation of localized "intelligence" and will provide the capability for exercising local autonomous action. These capabilities should be of benefit to any aerospace system design problem if component reliability can be assured. Traditional aerospace dogma is to favor reliability over new innovations, primarily because of the limited access for repair and the need for operation in extreme

*IBM Almaden Research Center, San Jose, California.

†Epion Corporation, Bedford, Massachusetts.

‡Center for Microtechnology, The Aerospace Corporation, El Segundo, California.

environments. As currently envisioned, future aeronautical and space systems will include passenger transports traveling at hypersonic speeds near suborbital altitudes and space missions that will be administered by using compact, fully integrated spacecraft "packages." These packages will roam the cold recesses of the solar system (i.e., NASA's Pluto-Kuiper Express Mission) or the "dusty" tail of a comet (i.e., NASA's Stardust Mission), or will orbit in large-number constellations around Earth or other planets, serving as communication or observation outposts. Implementing these new missions will require the development of novel materials and systems integration approaches that are specifically "engineered" to withstand harsh environments.

The development of novel materials will necessitate the development of material processing tools that can fabricate these new materials and package them alongside electronics. The laser is one such processing tool with unique advantages for materials modification. First, the laser is a nonintrusive, *in-situ* processing tool that can simultaneously perform several tasks, including serving as its own process monitor. Second, the laser is easily amenable to automation and is commonly used in processing situations where site-specific action is necessary. Third, delicate operations can be done with lasers, including atomic layer-by-layer removal by etching and controlled ablation techniques, site-specific surface oxidation, semiconductor dopant deposition and dopant drive-in, surface annealing, embedded interface processing, and pulsed laser deposition (PLD) of single-unit crystal films.[2] In essence, lasers have the capability for establishing a nonequilibrium chemical environment for materials processing. As a consequence, novel materials and microstructures can be fashioned.

In this chapter, we explore the laser material processing applications for microengineering technology. We present the processing steps that might be required for developing miniaturized systems fashioned of numerous materials (e.g., semiconductors, insulators, ceramics, polymers, diamond, metals). We also detail the micromachining processes that might be implemented for developing microstructures for the following:

- Fluid delivery channels
- Resonant high-Q structures
- Surface corrugations and special topologies
  - To direct light
  - For acoustic waves
- Surface texturing for enhancing
  - Catalysis
  - Aerodynamic flow
  - Tribology
  - Thermal conductivity

In addition, we present the laser deposition schemes for enabling the growth of various thin-film devices (e.g., ferroelectric materials for radio frequency [RF] circulators, dielectric optical coatings, solid lubricant coatings, high-temperature superconductor ceramics). Finally, we discuss the generic use of lasers in postassembly processing:

- Embedded interface processing
- Direct-write processing (deposition and etching)
- Cutting/trimming

The selected processing techniques that are explained in this chapter use the laser wavelength and unique optical properties to advantage rather than as a mere heating source. Conventional laser processing techniques, such as those used for macroscale cutting and welding applications, are not covered in this chapter. Also not covered are the techniques in which the laser is used as a

light source, namely, in photochemical curing of plastics or as a general exposure "tool." However, the use of the laser to "write" 3D microstructure images with a volumetric-exposure technique is discussed.

The general scope of this chapter is to present a tutorial review of the pertinent fundamental theories on laser material-interaction physics and a few detailed examples of laser processing applications. For more information, the reader is directed to the numerous excellent reviews and books that cover this information in greater detail.[3] The intended audience is an interdisciplinary group composed of the aerospace engineering community; the traditional material processing community; the thin-films growth community; and the microengineering community, which performs research in (1) microelectronics processing, (2) MEMS, (3) microoptical electromechanical systems (MOEMS), and (4) advanced packaging.

Specifically, this chapter is organized into the following sections. Following the introduction, Section 2 presents certain attributes of laser processing. Section 3 covers the physical principles of laser processing. Section 4 presents a general overview of the important subsystems found in typical laser processing stations. Section 5 is a brief overview of the utility and limitations of laser processing. Section 6 describes four microengineering application examples where laser processing is used. Section 7 outlines a specific case study for the development of a laser processing tool. Section 8 concludes with a brief overview of future trends and applications specific to aerospace systems.

5.2 Laser Processing

5.2.1 Attributes of Laser Light

The usefulness of lasers in materials processing and microengineering has its basis in the attributes of laser light compared to the light from conventional radiation sources.[4] The directed-energy nature of laser light is perhaps the most important of these attributes, because energy can be delivered to a surface in a contactless mode. This action-at-a-distance attribute eliminates both mechanical interaction with the surface and the need for maintenance or replacement of worn parts. Another attribute is the low beam divergence of laser radiation–typically less than a few milliradians in the far field. A low beam divergence permits tight focusing, which in turn allows for high intensity and increased spatial resolution. Yet another key attribute is brightness, defined as the laser power per unit area emitted into a unit solid angle. The high brightness often associated with lasers is important in providing high-intensity radiation to a surface. Finally, an attribute that may or may not be a factor in laser processing, depending on the particular application, is laser coherence. There are two types of coherence, spatial and temporal. Spatial coherence is of greater importance than temporal coherence, because it is related to the spatial mode structure of the laser and hence to the beam-focusing properties. Temporal coherence is closely related to the monochromaticity of lasers. Lasers enable high average power to be delivered in a narrow wavelength range, which permits a great deal of selectivity for surface processing. Although single-frequency operation is obtainable in certain lasers, rarely is this degree of monochromaticity required. What is more important is the capability to deliver energy in specific wavelength regions, such as the deep ultraviolet (UV) or mid infrared (IR). The importance of this capability will become clearer in later sections that describe existing laser applications.

5.2.2 Laser Parameters of Importance for Microengineering

Table 5.1 lists several key laser parameters and their general impact upon laser material processing. When using laser processing for a particular application, the first consideration is what wavelength (and thus what type of laser) to use. The wavelength determines the amount and efficiency

of laser radiation coupling to the material's surface, because a material's absorptivity and reflectivity are wavelength dependent. For example, the processing of metals is far more efficient (in terms of photon utilization) with UV light rather than with IR radiation because of the significantly reduced reflectivity in the UV. In addition, the wavelength influences the focused spot size because of the direct relationship between the minimum spot size and wavelength.

Once the wavelength is determined, the key parameter to consider in most applications is the laser intensity. Intensity, in typical units of W/cm^2, refers to the amount of energy delivered to the surface per unit area and per unit time. By increasing or decreasing the laser intensity, various types of physical processes can be made to occur. These processes include melting, vaporization, ablation, deposition, etching, and for some atomically selective processes, multiphoton excitation. For example, by increasing the laser intensity during pulsed irradiation of a metal surface, simple melting can give way to droplet ejection and ablation. There are several laser parameters that influence the laser intensity, which are also listed in Table 5.1. For instance, for continuous-wave (cw) irradiation, the average power and spot size directly affect the laser intensity. The spot size also determines the local processing area and the spatial resolution as defined by the heat affected zone (HAZ). Precisely focused laser beams are capable of irradiating micron-sized areas. Submicron-sized areas can also be selectively processed by using interferometric lithography techniques.[5] For pulsed operation, both the energy and duration of a single pulse directly affect the peak intensity of the focused beam. Often, for fixed-pulse-length applications, the fluence, rather than the intensity, becomes the figure of merit. Fluence is the delivered energy per unit area per pulse, and the units are in J/cm^2. The delivered number of pulses per second, or the pulse repetition rate, clearly influences the processing rate and the speed of an application. For volume manufacturing, the pulse repetition rate is the one parameter that determines the throughput and time efficiency of a process. For many materials, pulsed irradiation of the surface results in a transient temperature rise. If the material's thermal diffusivity is small, then this temperature rise may be sufficient to induce melting and vaporization. For situations where the pulse repetition rate is high enough, this transient heating effect can be accompanied by a subsequent bulk-material heating. To the extent that this heat affects the processing application, bulk heating may ultimately limit the resolution to areas much larger than the focused spot size.

Table 5.1. Laser Parameters for Microengineering Applications

Parameter	Impact
Wavelength	Radiation coupling efficiency to surface; spatial resolution.
Average power	Influences intensity, background heating.
Pulse energy	Influences peak intensity.
Pulse duration	Influences peak intensity, thermal diffusion length.
Focused spot size	Influences intensity, processing area, spatial resolution.
Intensity	Influences type and extent of surface processing.
Fluence	Influences type and extent of processing for pulse applications.
Pulse repetition rate	Influences processing rate, direct current (dc) heating.
Polarization	Influences coupling of energy to surface; process anisotropy.

Finally, another key parameter that affects laser processing is the polarization vector of the laser irradiation. Polarization may influence the degree of radiation coupling to the surface, and thus the uniformity of a particular type of processing. As an example, the quality of etching deep, high-aspect-ratio features in ferrites is affected by the polarization-dependent reflectivity of the sidewalls.[6]

5.2.3 Lasers for Microengineering

Since the invention of the laser in the early 1960s, literally hundreds of different types of lasers have been developed. It is safe to say that most of these lasers have had no influence on the commercial and military sectors. For materials processing and microengineering applications, there exist a few gas, solid-state, and metal-vapor lasers that are turned to again and again because of their inherent capabilities. Liquid-state dye lasers, never important for materials work, are disappearing because of rapid advances in tunable solid-state lasers.

The important lasers for microengineering work are listed in Table 5.2. Among the gas lasers listed, the ubiquitous CO_2 laser is the industrial workhorse. This laser is capable of providing cheap and plentiful photons in either pulsed or cw modes. Limitations of the laser are that the IR wavelength cannot be focused to micron-sized spots and that the coupling efficiency to a solid surface is often poor. Nevertheless, for the processing of certain materials (i.e., glasses), this laser is an excellent choice. Other lasers useful for microengineering are the rare gas ion lasers, such as Ar^+ or Kr^+, which provide powerful cw operation in the visible and UV spectral regions. These lasers are often used for scribing and deposition work, and can provide small intense spots because of their shorter wavelengths and good beam quality. The drawbacks of these lasers are their expensive electrical requirements and limited plasma tube lifetimes. The rare gas halide excimer

Table 5.2. Lasers for Materials Processing and Microengineering

Type	Laser	λ	Significance and Use
Gas	CO_2	9–11 μm	Pulsed and cw operation; low cost of ownership.
	Ar^+	Many lines	cw operation; strong green output; UV lines.
	Excimer	0.35–0.19 μm	Highest pulsed energy output in UV; significantly more expensive than CO_2; has revolutionized UV materials processing.
Metal vapor	Copper	0.51 μm	Short pulse, high pulse repetition frequency visible output that can be frequency doubled; unknown reliability in manufacturing setting.
	He-Cd	0.44 μm 0.32 μm	Blue and UV cw output; limited ion tube lifetime
Solid state	Nd:YAG	1.06 μm	Popular workhorse laser; cw or pulse operation; harmonics can be efficiently generated to create UV and visible radiation.
	Ti:sapphire	0.80 μm	Pulsed, tunable laser that can be efficiently frequency doubled; generator of femtosecond pulses.
	Diode	0.63–1.0 μm	Electrically efficient; pulsed or cw operation; low power and limited wavelength selection.

lasers, on the other hand, have caused a small revolution in laser processing ever since their invention in the late 1970s. The excimer lasers remain the only commercial source of high average power, deep UV radiation currently available. Their high pulse energy permits efficient etching and ablation of surfaces over relatively large areas. The UV nature of the radiation, coupled with the poor spatial coherence of the lasers, allows for speckle-free high-resolution patterning. Indeed, micron and submicron patterning applications have been routinely reported.[7] Excimers are the laser of choice for PLD applications, for reasons that will be discussed later in this chapter.

High-repetition-rate (>10 KHz) copper vapor lasers, which long suffered because of the reliability issue, have made a comeback as viable lasers for the micromachining of thick metals. Precision holes for automotive fuel injection systems are now being cut by these lasers. The visible wavelength of the lasers (517 nm) limits their applications. Copper vapor lasers can be frequency doubled to the UV (~258 nm), but the conversion efficiency is poor because of the multimode nature of the laser. On the other hand, cw He-Cd lasers, operating at two wavelengths (325 and 447 nm), have not been used much in micromachining applications. The output power of these lasers is low even though the wavelength of operation is useful. These lasers have found use in exposure and soft printing applications.

Solid-state lasers for materials processing are led by the Nd:YAG laser. This laser can be operated either in cw or pulsed mode at fairly high average powers. Unlike the CO_2 laser, the Nd:YAG can be efficiently converted to its harmonic wavelengths of 0.532, 0.355, and 0.255 μm, particularly when it is operating in a pulsed Q-switched mode. This wavelength conversion feature permits more flexibility in applications. For high pulse repetition work, the Nd:YVO_4 laser can operate at up to 100 kHz with excellent pulse-to-pulse stability. Another laser that is a relative newcomer to the solid-state group is the Ti:sapphire laser. The great advantage of this laser is its tunability near the fundamental wavelength of 0.8 μm. The Ti:sapphire laser can also be efficiently frequency doubled to provide tunable near-UV output. In addition, mode locking of this laser creates femtosecond pulses (10^{-15} s). There is increased interest in these very short pulses as a new and powerful means for performing laser-based microengineering.[8] Finally, diode lasers, with their small size and high electrical efficiency, are starting to be used for some types of laser processing. Diode lasers can operate in either cw or can be directly modulated to gigahertz rates. Because these single-spatial-mode lasers have relatively low power and limited wavelength range (0.6–1.0 μm), they are not widely used. However, continued advancement in diode technology promises more powerful lasers with a greater choice of wavelength in the future.

It is also worthwhile to mention the advent of the powerful free electron lasers (FEL). There is interest in such lasers for materials processing because of their ability to provide high average power radiation that is tunable over a wide spectral range.[9] Additionally, the high spatial quality beam emits picosecond duration pulses at megahertz rates. Thus, very high throughput operations are possible, even though the amount of material processed on a per-pulse basis may be small. Currently, these lasers are still in the experimental stage, and no FEL has yet emerged that can be considered as a viable candidate for radiation processing of materials. Nevertheless, a U. S. government-sponsored FEL program at the Thomas Jefferson National Laboratory in Virginia is commissioning a kilowatt class (37-MHz repetition rate) IR FEL designed for laser processing studies. The results from this machine should go far to discern the credibility of these lasers for industrial use.

5.2.4 Laser Material Processing Tools

Lasers as material processing tools are typically used to alter a material by exposure, ablation, or etching (the latter, by the addition of chemical reagents). Also, laser tools can grow a material by

redeposition of the ablated material, by the addition of chemical precursors to induce chemical vapor deposition (CVD), by the sintering of nanophase powders/slurries, or by the curing of polymers. In general, laser tools either operate via a batch-processing scheme, where the laser beam passes through a mask and irradiates a selected large area, or via a direct-write serial-processing scheme, where the laser beam is focused onto a specific small area. The former approach typically offers high throughput, while the latter approach offers site-specific processing control. In complex tools, a combination of masking and direct-write focusing is implemented to provide arrays of focal point sources for parallel processing. As a general rule, laser tools that employ masks are mostly designed for production, while those that implement direct-write action are used for rapid prototyping. This generality does not hold for laser welding or cutting applications, which are primarily direct-write tools. These applications are not discussed in this chapter but are deemed mature technologies found in many manufacturing industries.

For specific microengineering applications, both batch-processing and direct-write approaches are used, with the direct-write approaches offering more flexibility. Direct-write laser processing instruments typically include a laser beam delivery system (BDS) with a focusing microscope objective, a computer-driven XYZ stepper and/or optical scanners, and a surface imaging system to monitor progress. Additional modifications to the instrument may include the capability to process at multiple wavelengths; to measure the surface topography with a white-light or laser interferometer; and to continuously dose the surface with gas for etching, deposition, or debris removal. By employing the appropriate laser, a direct-write processing instrument can be used for etching materials, ablating materials, annealing materials, or depositing materials and dopants, all with site-specific control. There are two direct methods for removing material: chemical etching[10] and ablation.[11] The indirect method is by photoexposure.[12] Similarly, there are at least two techniques for depositing material: laser CVD[13] and PLD.[14] The PLD technique has at least two variants. One variant is known as MALDI (matrix-assisted laser desorption/ionization), and the other is called MAPLE (matrix-assisted pulsed laser excitation). These relatively new variants are primarily used to deposit intact large organic or biologically significant molecules. Direct-write laser techniques can be used for the micromachining of ceramics,[15] glasses,[16] and diamonds,[17] and for the deposition of polysilicon and semiconductor dopants. It is also possible to "drive in" the dopant[18] via laser irradiation. The ultimate resolution for the direct-write technique is normally subject to the limitations of diffraction. However, it is feasible to fabricate patterned lines that are less than the diffraction-limited spot size. For this fabrication, the coherent properties of the laser are exploited, and surface interference effects are taken to advantage. It is then possible to fabricate patterned lines in the ~ 0.1 μm range.[19] In general, and especially for micromachining applications, spot size and depth of focus are the critical parameters. As a consequence, material processing with short depth of focus requires a precise knowledge of the objective lens-to-surface distance. If the surface topology is corrugated, a servoloop connected with an interferometric autoranging device must be used.

5.3 Physical Principles of Laser Processing

5.3.1 Beam Propagation, Energy Delivery on Target, and Coherence

Under most laser processing conditions, the criteria for optimum interaction between the laser and the material are indicated by a handful of equations. These equations describe the propagation of the laser beam energy through the beam delivery optics, the photophysical interaction of the laser beam with the surface (i.e., absorption and surface chemical interactions), and the subsequent surface modification as a result of electronic and thermal excitation. The equations are simplified for a Gaussian laser beam propagating in a diffraction-limited optical system, though for most

material processing, a top-hat or flat-top homogenized beam is used.[20] A Gaussian beam can be described by the radius function $\omega(z)$ and the wavefront curvature function $R(z)$ along the propagation direction z. The functions $\omega(z)$ and $R(z)$ are given by Eqs. (5.1)–(5.3)[21]

$$\omega^2(z) = \omega_o^2\left[1 + \left(2\frac{z}{b}\right)^2\right] \tag{5.1}$$

$$R(z) = z\left[1 + \left(\frac{b}{2z}\right)^2\right] \tag{5.2}$$

$$b = \frac{2\pi\omega_o^2}{\lambda} \tag{5.3}$$

where λ is the wavelength, ω_0 is the beam radius at the waist, and b is the confocal parameter (i.e., distance within which the diameter of a focused beam remains nearly constant, $-b/2 < z < +b/2$). The Gaussian beam contracts to a minimum diameter $2\omega_0$ at the beam waist, where the phase front is a plane wave.

Consider a collimated and strongly focusing Gaussian beam with the criteria that 99% of the energy is to be transmitted by the focusing lens of focal length f through an aperture D, and 86% of the energy is to be contained within a diameter $d_o = 2\omega_0$. The spot size d_o for this beam is given by Eq. (5.4).[22] Equation (5.4) can be recast using the more familiar $f^{\#}$ (where $f^{\#}$ is called the f-number and is defined as (f/D). Given a fixed focal length lens, a smaller d_o means shorter wavelengths and larger Gaussian beam diameters at the lens.

$$d_o \sim \frac{2f\lambda}{D} \rightarrow 2f^{\#}\lambda \tag{5.4}$$

Lenses with $f^{\#} > 2$ are relatively inexpensive, while lenses with $f^{\#} < 1$ are commonly multielement designs and very expensive. The depth of focus for this Gaussian beam is given by the confocal parameter, b, given in Eq. (5.3), but can also be approximated as $\sim 2\pi(f^{\#})^2\lambda$. With the use of a 248-nm wavelength laser beam and a focusing lens of $f^{\#} = 2$ (i.e., $f/2$ optics), the result is a minimum spot diameter of ~1 μm and a depth of focus of ~ 6 μm for processing in air. If the medium in contact with the surface is in a higher index material, the minimum spot size is further reduced by the index n. In the example given above, 86% of the incident energy is focused onto the minimum diameter spot (1 μm), which leaves 14% of the energy distributed over a diameter of ~2.3 μm. The 14% energy "spillover" may be damaging for some micromachining applications. To guarantee greater than 98% energy confinement within the design spot size, Eq. (5.4) should be multiplied by 2.3. There are practical reasons why a very small $f^{\#}$ may not be desirable for some micromachining applications. With decreasing $f^{\#}$, the minimum spot size declines by the same factor, as opposed to the depth of focus, which declines by the larger factor, $\pi(f^{\#})^2$. Material processing with a very short depth of focus requires a very flat surface, or a servoloop connected to an interferometric autoranging device to maintain the focus as the sample is moved.

As discussed previously, spot size and depth of focus are the two critical parameters for a micromachining application. In an imaging application (e.g., image projection, photolithography), these parameters are the resolution and the depth of field. Equation (5.5) defines the resolution, R, of a diffraction-limited imaging system,[23]

$$R = \frac{C\lambda}{N.A.} \tag{5.5}$$

where C is a constant (derived from the first Fraunhofer diffraction minimum for a circular aperture) and is related to the coherence of the illumination source. The value of C goes from 0.61 (incoherent illumination) to 0.77 (coherent illumination). The *N.A.* is the numerical aperture $\equiv n\sin\theta_{max}$, where n is the index of refraction and θ_{max} is 1/2 the maximum acceptance cone angle, which specifies the "light-gathering power" of an optical system. A low *N.A.* has a value of ~0.25, while a high *N.A.* is ~ 0.5 (e.g., Schwarzschild lens[24]).The depth of field for such an imaging system is given by Eq. (5.6).

$$Z = \frac{\lambda}{(N.A.)^2} \tag{5.6}$$

Again, the *N.A.* emphasizes the inverse relationship between the need for high resolution and a practical depth of field. Equations (5.4)–(5.6) show that the shorter the wavelength, the better the resolution and the smaller the minimum spot size achievable, which argues for using UV over IR light. However, materials show increasing dispersion in the index n at the shorter wavelengths ($dn/d\lambda$), especially in the deep UV. For transmissive optics, this dispersion results in chromatic aberration in the focusing/imaging, which must be taken into account for UV laser sources with large spectral bandwidths. Current UV excimer lasers without injection-locking wavelength stabilization have bandwidths that make less than half-micron processing difficult. The defocusing error df as a function of the source bandwidth is given in Eq. (5.7).[25]

$$df = \left(\frac{dn}{d\lambda}\right)\Delta\lambda\frac{f}{(1-n)} \tag{5.7}$$

Table 5.3 presents the measured dispersion for fused silica for the excimer laser wavelengths, and the maximum allowable source spectral linewidth, $\Delta\lambda_{max}$, for achieving a defocusing error of less than 1 μm, given a $f = 1$ cm lens.[25] Current excimer laser linewidths are typically 0.8 nm for wavelengths at 248 nm. Injection-locking schemes are used to narrow the emission linewidths, $\Delta\lambda$, to < 0.003 nm and thereby also to reduce the defocusing errors.

Table 5.3. Dispersion Values for Fused Silica, $dn/d\lambda$, for Achieving a Defocusing Error of Less than 1 μm, Given a $f = 1$ cm Lens, $\Delta\lambda_{max}$

	193 nm	248 nm	308 nm	351 nm
$dn/d\lambda$ ($\times 10^{-4}$ nm^{-1})	8.9	6	3.2	1.8
$\Delta\lambda_{max}$ ($\times 10^{-2}$ nm)	6	8	16	29

Fundamentally, a reduction in the laser linewidth means an increase in the coherence properties of the laser. In essence, it means maintaining the distinct time and phase relationship of the emitted photon wavetrains. In general, the coherence properties of a laser are delineated as arising from either the spatial or temporal domain. In spatial coherence, for any extended optical source, optical wavetrains can originate from spatially separated points. For lasers, the phenomenon is related to the number of laser transverse cavity modes that can extract energy from the gain curve. Reducing the number of operating cavity modes increases the spatial coherence. In temporal coherence, the coherent emission of light from atoms has finite duration, $\Delta\tau$, and consequently a finite frequency distribution spread, $\Delta\nu$ (i.e., finite bandwidth as a result of these truncated sinusoidal wavetrains). For pulsed lasers, the phenomenon is related to the pulse width of the laser (i.e., the duration of the population inversion); the atomic energy decay modes; and the average

number of times the laser energy is allowed to recirculate prior to exiting (i.e., cavity round-trip times). Of the two coherence properties, the spatial coherence influences the imaging and focusing capabilities of the laser beam, while the temporal coherence could induce novel photochemical or photophysical processes on surfaces or in bulk media. In practicality, the spatial coherence is more important than temporal coherence, and most precision processing lasers operate only in the fundamental transverse electromagnetic mode TEM_{00} (i.e., lowest order self-reproducing hermite-Gaussian cavity mode). Maintaining the spatial coherence of a laser also requires that the paraxial optical BDS be specially designed to match the confocal parameter of the laser with that of the cascading transfer optics.

In general, most pulsed lasers are best described as partially coherent sources, while cw lasers can be designed as nearly perfect coherent sources. The temporal coherence property of pulsed lasers is typically given by the coherence length, l_c. The l_c defines a distance, usually measured from the exit window of the laser, where the laser electromagnetic field amplitude and phase front changes in a consistently predictable way. In effect, the laser is considered a temporally coherent source for interactions at a distance less than l_c. Using the time-bandwidth product theorem, or Heisenberg uncertainty principle (which states that $\Delta\nu\ \Delta\tau \sim 1$, where $\Delta\tau$ is the laser pulse width and $\Delta\nu$ is the spectral bandwidth), the corresponding coherence length l_c is given by Eqs. (5.8) and (5.9). In these equations, the c is the speed of light, and λ, ν are wavelength and frequency, respectively.

$$l_c = c\Delta\nu \approx \frac{c}{\Delta\nu} \tag{5.8}$$

given that $c = \lambda\nu$ and $\Delta\nu = (c/\lambda^2)\Delta\lambda$

$$l_c \approx \lambda\left(\frac{\nu}{\Delta\nu}\right) \text{ or } \approx \frac{\lambda^2}{\Delta\lambda} \tag{5.9}$$

Current state-of-the-art solid-state lasers with injection-seeded oscillators have typical spectral linewidths of 50 to 90 MHz. For example, a Nd:Yag laser operating at a laser wavelength of 1064 nm with a spectral linewidth of 90 MHz gives a coherence length of 3.3 m. Novel nonthermal processing of materials would be possible within this coherence length. Because most of these lasers have a pulse width of 10 ns, which corresponds to an optical length of ~ 3.3 m, laser photons from the leading edge of the pulse would be coherent in relation to laser photons at the trailing edge of the pulse. Examples of nonthermal processing include the coherent "driving" of energy into excitonic particles and surface electrons.

5.3.2 Processing Speed and Process Window

There are cases in laser material processing where the laser repetition rate or the stepper/scanner speed is not the limiting factor. In such cases, the processing throughput is determined by the fundamental process speed, Ω_{sp} (μm/s). The Ω_{sp} depends on many factors, but is intrinsically dependent on the fundamental photophysical interaction (e.g., electronic, thermal, plasma); the character of the surface under irradiation; and the properties of the incident laser light. The photophysical interaction is a function of the laser fluence (J/cm^2) or the intensity (W/cm^2). In general, at very low fluences, the photophysical process is primarily induced by electronic excitations; at intermediate fluences, by thermal processes; and at high fluences, by the above-surface laser-initiated plasma. Similarly, the morphology of the surface changes with increasing laser fluence. In general, at low fluences, there is surface and near-surface defect formation; at intermediate fluences, there is surface melting and rapid recrystallization, resulting in amorphization; and at high fluences, there is plasma sputtering, spallation, and shock-induced damage. For all laser

fluences, knowledge of prior irradiation dose is critical to predicting additional surface changes. Therefore, for controlled processing, the photophysical interaction must be maintained within the domain of interest. Table 5.4 displays pertinent photophysical processes and the factors that impact laser processing. The table illustrates the many factors that characterize a process window and ultimately the processing speed, Ω_{sp}. A process window is characterized by measurement of the phenomenological processing rate, Γ (e.g., μm/s of material etched, ablated, or deposited). A simple model can be derived to relate Ω_{sp} to Γ. Assume the laser spot size diameter on the workpiece is D(μm) and the required processing thickness is ℓ(μm) (i.e., material to be etched, ablated, or deposited). Then ℓ/Γ gives the time to process one spot size. The stepper/scanner must move a distance D per ℓ/Γ unit time. The stepper/scanner speed or material processing speed is then given by Eq. (5.10):

$$\Omega_{sp} = \left(\frac{D}{\ell}\right)\Gamma \tag{5.10}$$

Lasers can be used for etching, annealing, or forming "luminescent silicon."[26] The projected processing speeds depend on the laser parameters and the experimental conditions employed, as follows:

- Type of laser (cw or pulsed)
- Laser wavelength
- Processing technique or chemistry employed (e.g., chlorine-etch or ablation)
- Laser polarization vector with respect to the scan direction (i.e., E ||: parallel or E⊥ perpendicular)

For example, a cw laser (Ar^+ ion) operating at 514 nm with 1.5 W output power, with a chlorine base etch chemistry and polarization set to E||, can cut 5-μm-deep trenches in silicon with a

Table 5.4. Photophysical Processes Used in "Direct-Write" Laser Processing, and Critical Factors

Photophysical Processes	Critical Factors
Chemical (deposition/etch)	Reaction initiator (gas phase absorption or substrate absorption) Optical absorption coefficient Heterogeneous reaction rate at gas-solid interface Diffusion of reactants/products (mass transport) Substrate thermal conductivity Nucleation rate Point and line defect densities
Ablation	Laser fluence and intensity Irradiation dose Surface morphology Bulk defect density Thermal conductivity (thermal diffusion length)
Laser-induced desorption	Wavelength Optical absorption coefficient Adsorbate binding energy Fluence and intensity Point defect density Metals (excited plasmon density)

process speed, Ω_{sp}, of several millimeters per second.[27] For the opposite polarization, the etching rate is a factor of 2 slower and results in nonuniform etching of the sidewalls. For pulsed laser ablation (excimer laser, 248 nm, 1.3 J/cm^2, 5 Hz repetition rate), a Ω_{sp} of 0.6 mm/s has been achieved with hole depths of 150 μm.[28] In comparing the laser-assisted chlorine-etch technique with the ablation technique, the former produces a smoother lined wall,[29] but the latter has a wider dynamic range of trenching depth.

The Γ for numerous materials and laser processes (e.g., semiconductors, insulators, and metals) can be found in the literature.[30] Because the process conditions influence Γ, one expects different Γ for different laser irradiation conditions (see Table 5.1). Gas dynamics also influence Γ. For example, for process windows where Γ is limited by the diffusion of reactants or products into and out of the processing zone, using smaller spot sizes can lead to an increase in Γ by factors approaching 10^4. This increase is primarily a result of diffusion geometrics. As the spot size is *reduced,* there is a transition in the reactant, and product diffusion from a 3D expansion process to a one-dimensional (1D) process. A consequence of the reduced dimensionality is that the reaction fluxes in the active zone increase, resulting in an effective larger Γ. For laser-assisted chemical processing, the transition from 1D to 3D expansion appears for spot sizes near 80 μm.[31]

Diffusion-limited processing can be deleterious to the fabrication of high-aspect-ratio structures (hole-depth/hole-width » 1), because mass transport to and from the active zone is limited. The derived simple processing speed model, as shown in Eq. (5.10), is not valid and must include parameters for diffusion. Equation (5.11)[32] relates Ω_{sp} to Γ for processing in the diffusion-limited regime. The L is a constant related to the diffusion properties of the product. Equation (5.11) reduces to Eq. (5.10) for small l/L ratios.

$$\Omega_{sp} = \frac{D\Gamma}{L}\left[\exp\left(\frac{l}{L}\right) - 1\right]^{-1} \tag{5.11}$$

Processing speed, Ω_{sp}, is also influenced by light scattering out of the active zone or waveguiding into and out of an active zone. For example, if the material is processed via a cw or long pulse laser and the products include cluster particles, then the intensity at the processing interface could be reduced as a result of the light shadowing or scattering from the ejecta. The Mie scattering theory applied to large opaque particles (with diameters $\approx\lambda$) shows that the loss of laser energy is proportional to twice the particle diameter. Another effect in the laser fabrication of high-aspect-ratio structures like deep (>50 μm) via holes is that of waveguiding[33] by total internal reflection. Figure 5.1 shows the condition and gives the threshold condition based on Brewster's angle. Note that the in-plane (p) polarized light is not reflected but is absorbed at the wall, resulting in sidewall nonuniformity. For ℓ/D ratios resulting in $\varphi > \varphi_{Br}$, total internal reflections within the trench should be expected. Under these circumstances, great care must be exercised in aligning the laser polarization angle.[34]

5.3.3 Optical Absorption, Thermophysics, and Laser-Induced Plasmas

The fundamental laser–material interaction is nominally governed by the optical absorption of the material. Leaving out certain specifics, this absorption can have bandwidths (1) with near-molecular origin (<cm^{-1}), as for certain adsorbates; (2) more akin to the band structure of solids (>>cm^{-1}), as for periodic lattice crystals; or (3) near continuum absorption, as for a free-electron gas metal or a plasma. In the first and second cases, spectroscopic measurements define the absorption properties, while in the third case, specific models and the material dielectric properties can be used to get general absorption behavior. For example, the optical properties of metals are derived from the dielectric constant. At laser wavelengths where a metal behaves like an ideal free-electron metal, its dielectric properties can be approximated by the Drude model.[35] The

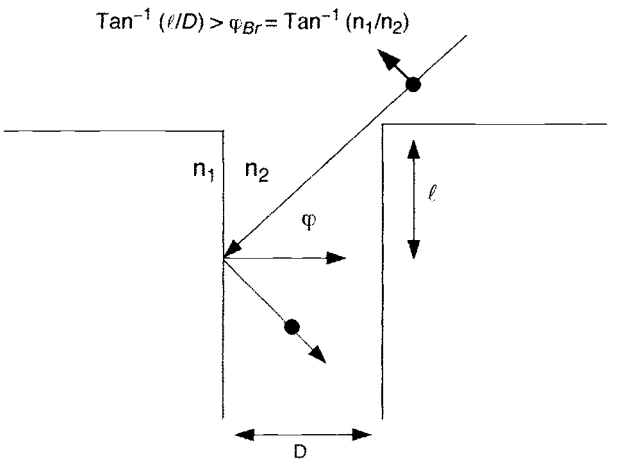

Fig. 5.1. Impact of Brewster's angle on laser "via hole" drilling. Total internal reflections occur for $\varphi > \varphi_{Br}$.

dielectric constant ε is temperature dependent and can be related to the angle-dependent reflectivity, R. Equations (5.12) and (5.13) describe the change in reflectivity for the transverse electric ([*TE*]–vector perpendicular to plane of incidence, or typically identified as s-polarized) and the transverse magnetic ([*TM*]–electric vector parallel to plane of incidence, or typically identified as p-polarized) polarized waves as a function of incident angle θ. The angle θ as defined is relative to the surface normal. At normal incidence ($\theta = 0$), the *TM* and *TE* reflectivities degenerate into one equation which, for completeness, is given in Eq. (5.14). The n and k are the real and imaginary parts of the complex index of refraction. They are related to the dielectric constant by the equation $\varepsilon^{1/2} = n + ik$. The extinction coefficient, k, is related to the optical absorption coefficient $\alpha(\text{cm}^{-1})$, as given by Eq. (5.15). Equation (5.15) also defines the optical absorption coefficient and the resulting attenuation of the laser intensity (I) over a distance (z).

$$R_{TM} = \frac{\cos(\theta) - \cos(\theta)/\varepsilon^{1/2}}{\cos(\theta) + \cos(\theta)/\varepsilon^{1/2}} \tag{5.12}$$

$$R_{TE} = \frac{\cos(\theta) - \varepsilon^{1/2}\cos(\theta)}{\cos(\theta) + \varepsilon^{1/2}\cos(\theta)} \tag{5.13}$$

$$R_{(TM)/(TE)} = \frac{(n-1)^2 + (k)^2}{(n+1)^2 + (k)^2} \tag{5.14}$$

$$\alpha = \frac{4\pi k}{\lambda} \tag{5.15}$$

where $dI(z)/dz = -\alpha I$.

Regardless of the initial absorption process, the absorbed energy quickly spreads via numerous decay channels and results in bulk heating. However, there are cases where the deposition of energy in a specific absorption feature induces a specific action without the consequences of heat. These nonthermal phenomena are generally observed in femtosecond laser pulse experiments[36] or in low-fluence laser material interaction experiments.[37] In both sets of experiments, the material is "processed" on the atomic scale with processing yields so low that, as a processing technique, is of minimal use for practical applications. However, with ever-increasing laser repetition

rates (kHz → MHz), low-yield, species-selective processes can be viable for certain applications where atomic level of control is necessary. Nevertheless, for most laser material processing, the consequences of bulk sample heating by the laser must be considered because this heating can influence the processing resolution or the fabrication throughput. The time scale and the nature of the heat flow characterizes the type of processing. For long processing times (i.e., which result with the use of cw lasers), the temperature distribution is in steady state and the heat flow problem is only tractable via a 3D solution. A practical consequence of operating in this heating domain is that the effect of high temperature on adjacent features needs to be taken into account. In contrast, for short processing times (i.e., which result with the use of short-pulse lasers), the heat flow is primarily a 1D problem, where the temperature gradient is into the bulk and normal to the surface. Under these conditions, the effect of high temperature on the surrounding area can be ignored. Because lasers can induce a wide range of heating rates–up to as high as 10^{15} K/s (femtosecond pulse excitation)–the processing thermophysics is governed by the thermal properties of the irradiated material. These properties include the thermal conductivity [(κ; W/(cm-K)], the heat capacity [c_p; J/(cm^3-K)], and the temperature-dependent optical properties. Equation (5.16) defines the thermal diffusion length (in cm), where τ is the processing duration (i.e., the laser pulse duration). The ratio (κ/c_p) is called the thermal diffusivity, D_T (cm^2/s), and can be used to calculate the time for reaching a steady-state temperature within a processing zone of size ψ. This time is given by $T \approx \psi^2/(4D_T)$.

$$\chi = \left(\frac{4\kappa\tau}{c_p}\right)^{1/2} \tag{5.16}$$

Using the metals as an example, the optical absorption depth ($1/\alpha$) for most metals, in the visible and the near-IR regions, is only a few hundred angstroms. On the other hand, for nanosecond pulsed lasers, the thermal diffusion length, χ, is on the order of 1 μm. So for most *pulsed* laser processing of metals, the optical absorption depth is much shorter than the thermal diffusion length ($1/\alpha < \chi$). Under these circumstances, the temperature at the material surface can be calculated if the laser pulse shape is known.[38] However, for the purpose of material processing, the key issue is whether the thermal diffusion length, χ, is greater or less than the feature size, ψ, to be processed; likewise, if the processing time, ψ/Γ, for the feature is greater or less than $T \approx \psi^2/(4D_T)$. If the *processing time is greater* than T, then the solution requires a 3D analysis in which the laser intensity radial distribution must be identified. The 3D analysis is complicated, but for a circular aperture and a cw irradiation zone, the affected area is a hemisphere of diameter $(\pi\psi)^{1/2}$. On the contrary, if the *processing time is less* than T, then the heat diffusion is a 1D problem, and the maximum temperature rise at the surface, ΔT_{max}, can be approximated by Eq. (5.17).[39]

$$\Delta T_{max} = \frac{F(1 - R_{sol})}{c_p \chi} \tag{5.17}$$

where F is the laser fluence (J/cm^2) and R_{sol} is the surface optical reflectance. The numerator on the right-hand side of the equation describes the laser fluence absorbed. In most cases, the thermochemistry is governed by the temperature fall time, which is given by $\Delta T_{fall} \sim \chi^2/(4D_T)$.[39] For weak absorbing materials where $1/\alpha > \chi$, $1/\alpha$ replaces χ in Eq. (5.17) and in the equation for ΔT_{fall}. In the particular case of weak absorbers (i.e., wide bandgap insulators or semiconductors) or thin films, the laser material interaction may create defects[40] in the material or may infuse stress or strain in both the irradiated and surrounding area.[41] To analyze the stress and strain distribution, the material thermoelastic equations must be solved to quantify the effect of the laser heating.[42] An understanding of the residual stress is important for implementing the laser

annealing technique[43] or any laser direct-write processing technique. The annealing irradiation dose and the scan speed have an effect on the residual stress distribution. A highly stressed material commonly quenches by atom dislocation and microcracking, while a low stressed material shows a shift in the phonon spectrum. In both cases, the material is ridden with defects, which can be used to advantage to induce particle emission from the surface via a nonthermal laser excitation scheme.[44,45]

The description of the laser material interaction, as given by the optical absorption and subsequent thermal processes, is valid as long as the photoejected species density is small. With increasing laser fluence, more material evaporates and the likelihood for photoionization and thermionic emission[46] increases. The Richardson-Smith equation estimates the thermionic ion emission current as a function of temperature.

$$J_+ = A_p T^2 \exp[-(I_p + \varphi_o - U_{ce})]/kT \tag{5.18}$$

In Eq. (5.18), A_p is a constant, T is the local temperature, I_p is the ionization potential (eV/atom), φ_0 is the electron work function (eV), and U_{ce} is the cohesive energy (eV/atom). With further increase in the laser fluence, both the photoionized and the photoemitted electrons absorb energy from the laser beam via the inverse Bremsstrahlung process. The absorption process is described as a three-body interaction with nearby ions and raises the electron to a higher electronic state. The higher kinetic energy electron ionizes additional atoms via electron impact excitation. The resulting effect is an avalanche of ionization with less light actually delivered to the target and more light into the protoplasma. The absorption coefficient for the Bremsstrahlung process can be calculated and is given in Eq. (5.19) in cgs units.[38]

$$K_\nu = \left(\frac{4}{3}\right)\left(\frac{2\pi}{3kT}\right)^{1/2} \frac{n_e n_i Z^2 e^6}{hcm^{3/2}\nu^3}\left[1 - \exp\frac{-h\nu}{kT}\right] = 3.69 \times 10^8 \left(\frac{Z^3 n_i^2}{T^{1/2}\nu^3}\right)\left[1 - \exp\left(\frac{-h\nu}{kT}\right)\right] \tag{5.19}$$

where n_i and n_e are, respectively, the ion and electron densities in a plasma of average charge Z and temperature T. The c, e, m, h, and k are, respectively, the velocity of light, the electronic charge, the electron mass, Planck's constant, and Boltzmann's constant; ν is the frequency of light that is related to the wavelength by the equation $c/(N\lambda)$ (where N is the plasma optical index). The term $1/K_\nu$ defines the light absorption pathlength (cm) into the plasma, while the term $[1-\exp(-h\nu/kT)]$ accounts for losses by stimulated emission. For specific conditions, Eq. (5.19) can be approximated. For $h\nu >> kT$ (e.g., UV wavelength laser), the $K_\nu \sim (T^{1/2}/\nu^3)^{-1}$ while for $h\nu << kT$ (e.g., high-temperature plasma), the absorption coefficient is approximated by $K_\nu \sim (T^{3/2}\nu^2)^{-1}$. All other parameters being equal, in both extreme cases, the shorter wavelength laser is preferable because it results in a smaller K_ν. If the laser fluence is such that an above-surface plasma does form, then only optical frequencies higher than the plasma frequency, $\nu_p = 8.9 \times 10^3 n_e^{1/2}$, can penetrate the plasma. Conversely, given a laser with frequency ν, the laser can penetrate the plasma for electron densities $n_e < (\nu/8.9 \times 10^3)^2$.

The plasma temperature T, which appears in Eq. (5.19), is difficult to measure for a plasma that is not in local thermodynamic equilibrium. However, where thermodynamic equilibrium can be assumed (e.g., for long pulse width lasers or for laser-induced plasma densities), the temperature can be determined by spectroscopic measurement of the emission intensities and the coupled Saha equations.[38] Regardless, a laser-induced plasma absorbs power from the laser. The absorbed power is reradiated primarily via the Bremsstrahlung or lost via the plasma thermal conductivity. For processing on the micrometer scale, the result is a reduction in resolution. On the other hand, for processing on the macroscopic scale, the plasma can be "tailored" to deliver maximum energy

transfer to the material surface.[47] The reradiated power per volume (W/cm^3) is given in Eq. (5.20), and the thermal conductivity (W/cm^{-1} K^{-1}) is given in Eq. (5.21).[38] For completeness, Eq. (5.22) shows the time for equilibrating the electron and ion temperatures. The term ($ln\ \Lambda$) is a function of plasma parameters[48] and is of the order of 10, and A is the ion atomic weight in amu.

$$P = 1.42 \times 10^{-34} Z^3 n_i^2 T^{1/2} \tag{5.20}$$

$$\kappa = \frac{1.95 \times 10^{-11} T^{5/2}}{Z \ln \Lambda} \tag{5.21}$$

$$\tau_{eq} = \frac{252 A T^{3/2}}{n_e Z^2 \ln \Lambda} \tag{5.22}$$

Assume a laser irradiates an aluminum surface with spot diameter of 1 μm. Assume also that the fluence is such that a plasma temperature of 2×10^4 K (~1.7 eV) is established with $n_i = n_e \sim 10^{17}$ cm^{-3}. (Also assume it is a weak plasma roughly 0.001% of solid-state density, or ~1% vapor density at 1 atm.) For a 10 ns pulse laser, the plasma thickness is ~2.7×10^{-3} cm (~2.7×10^{-7} cm for a 1 ps laser), which results in a volume of ~2×10^{-11} cm^3 and a total reradiated power ~1 μW. The thermal conductivity of this plasma becomes ~ 10^{-2} Wcm^{-1}K^{-1}, which is similar to the thermal conductivity of an insulator (e.g., titanium dioxide [TiO_2]). The time for establishing temperature equilibrium is $\tau_{eq} \sim 0.1$ ns. Now consider increasing the ion and electron densities by a factor of 100. The power reradiated from the small volume increases by 10^4 (10 mW), while the time for reaching equilibrium decreases by 100 (1 ps).

5.4 Supporting Systems in Laser Processing

5.4.1 Beam Delivery System

There is a great deal of information on laser BDS. This information is covered to some extent in most papers dealing with laser processing.[50] In its essence, a BDS manipulates the laser beam such that the beam is delivered to its intended target with the desired spatial, temporal, and intensity characteristics. The components of a BDS include the familiar mirrors, lenses, attenuators, beam splitters, shutters, and polarization elements. Often, gimballing, translation, rotation, and angular adjustments of optical elements are required for the BDS; therefore, the instrumentation to perform these functions is usually included on the list of components.

Prior to establishing a BDS, the user must have thorough knowledge of the laser system and its purpose. Specifically, the usual laser parameters must be known (wavelength, beam diameter or size, beam divergence, pulsed or cw operation), along with the intended spot or image size and the required surface-incident intensity. This knowledge can then be used to establish the number and type of optical components needed to accomplish the task. Correct placement and use of the optical components of course requires a working knowledge of optics. Possible damage to the optic or its coating from the laser must also be assessed, particularly for short pulse or deep UV systems.

Two types of BDSs will be discussed: image projection and focused scanning. Although the BDS comes in many forms, these two represent generic types that are commonly used. Figure 5.2 shows an image projection system, while Figure 5.3 is a focused scanning system. Note that in the focused scanning system, it is the target, rather than the laser beam, which moves.

Image projection systems are often used with excimer laser processing to take advantage of that laser's high-resolution capabilities, and because the poor mode quality of most excimer lasers does not favor small spot focusing. Indeed, the multimode operation of the excimer laser lends

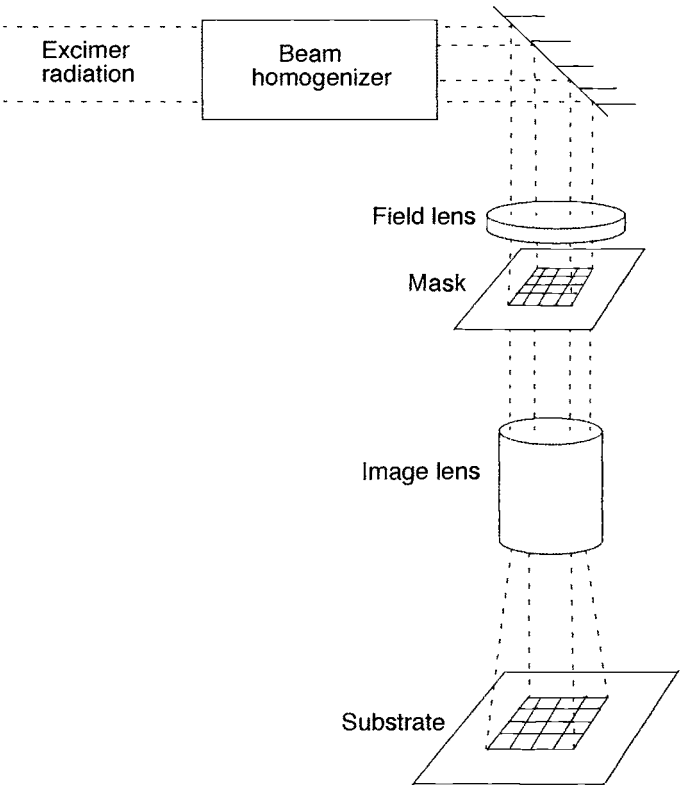

Fig. 5.2. Optical schematic of via ablation tool.

itself nicely to speckle-free imaging, which is one reason these lasers are in such demand for ultralarge silicon integration (ULSI) photolithography. The standard optical configuration for image projection is a Kohler illumination system.[51] As depicted in Fig. 5.2, the laser beam is often shaped before it enters a beam homogenizer. This ensures efficient photon utilization so that all the energy is captured by the homogenizer. In Fig. 5.2, a pair of anamorphic lenses are used in a telescope configuration to produce a square beam from an initially rectangular one. Because of the poor mode profile, most excimer beams have insufficient uniformity for projection processing. Beam homogenizers are then used to improve the spatial uniformity to the desired level.[52] Uniformity variation of less than 5% is often acceptable. Homogenizers function by producing a uniform plane of light just at their output. As the beam propagates, the spatial divergence significantly reduces the uniformity. Therefore, a field lens is used to image the uniform output plane from the homogenizer onto the aperture or mask. Note that the magnification of this lens does not have to be unity, but may either enlarge or diminish the beam size at the mask relative to the exit plane of the aperture. Once the mask is uniformly illuminated, a high-quality, low-aberration transfer lens is used to image the mask onto the intended target. The transfer lens typically possesses a magnification of unity or larger. Larger magnifications (2×, 5×, 10×) are often used in order to reduce the fabrication complexity (and thus cost) of the mask. As with all projection systems, the numerical aperture of each optical component must be matched with each of its neighbors in the optical pathway so that all energy is collected and no beam "spillover" occurs. A complete BDS can automatically locate the target in three dimensions (spatial positioning and focus).

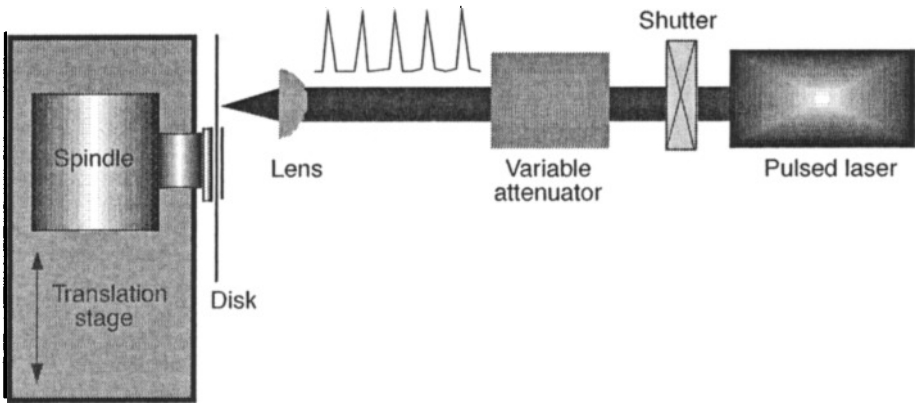

Fig. 5.3. Representative schematic of a focused laser direct-write processing system.

The BDS also includes display systems that permit real-time viewing of the part being processed. Such a camera system is often coupled with a high-quality microscope, so that micron-to-submicron patterns can be examined. The entire optical system (mask, projection lens, and target surface) must be rigidly mounted to prevent relative motion between these parts. The prevention of relative motion becomes all the more critical as the image size decreases.

For systems that possess good single-mode quality, the focused scanning BDS is a possibility. This type of BDS is possible because single-mode lasing permits a tight, well-defined focal region to interact with the surface of interest. Focused scanning systems are used in applications requiring extremely rapid beam movement or in the processing of very fine resolution patterns. Beam movement over a predetermined area is achieved by the mechanical motion of the beam under the programmed control of mirrors, prisms, or other special optics. As shown in Fig. 5.3, a single high-quality lens is used to focus the beam on the material surface. The spot size of the focused beam is controlled not only by wavelength, but also by the numerical aperture of the lens [see Eqs. (5.1)–(5.7)].[53] Because it often is easier to change the beam diameter (i.e., by varying an aperture, D) than the wavelength, a two-lens beam-expanding or beam-diminishing telescope is placed before the focusing lens to vary the focal spot size. Note that rarely are diffraction-limited conditions realized.

Intricate lines and patterns can be drawn by rastering the focused beam over the material surface. There are many ways to raster a beam. Figure 5.3 displays a scheme in which the focused beam is stationary, while the target substrate simultaneously rotates and translates beneath it. This scheme is but one of several techniques for moving the target. There exist many high-quality stages and substrate holders that can be moved and positioned with submicron accuracy under computer control. For systems in which the target cannot be moved, beam scanning can be performed by a variety of methods that fall into two general categories: those in which the focusing lens is placed before the beam-scanning optics, and those in which the beam-scanning optics are placed before the lens. The former category typically requires a long focal length lens to permit space for the scanning device between the lens and the target. Two examples illustrate these options. In the first example, two mirrors–one x-axis oriented and the other y-axis oriented–are used in an oscillating or gimballing motion to produce a "Lissajou-" type pattern on the material surface. In the second example, a rotating polygonal mirror is interposed between the lens and the target. As the mirror rotates, a beam is linearly scanned across the target. Angular adjustment of the polygonal mirror, at a rate much slower than the rotation rate, permits a series of parallel lines

to be drawn on the material surface. When a long focal length lens cannot be used, the scanning mechanism can be placed before the lens. However, the field of view of the lens must be sufficiently large to maintain focus as the beam "wanders" over the surface of the lens. Typically, the lens diameter is larger when the scanning mechanism is first than when the lens is first.

The above examples of BDSs have been for flat target surfaces. For curved and nonflat surfaces, optical components such as toric mirrors, axicons for generation of annular beams, and field-curving lenses can be used for processing.

5.4.2 Alignment, Positioning, Focusing

Alignment and positioning of a part or surface go hand in hand. Usually, it is necessary to consider the means for positioning prior to worrying about correct alignment. In general, positioning refers to the ability to move the part to meet requirements for movement in multidimensions with distance, velocity and acceleration, and incremental resolution criteria. Closed-loop control systems are often used with positioning systems to allow computer-controlled feedback and movement timing. Most positioning systems rely on x-y positioning tables, although commercial fixtures exist for rotational and angular motion. The size and weight of the workpiece dictate the size and choice of the motion system, because the mass of the part provides the inertia the positioning system must overcome. For applications of interest in this chapter, such as micromachining, semiconductor processing, and laser microchemical processing, highly precise lightweight motion tables are used. The x-y tables are composed of carriages and drivers (usually electric) that execute the motion in the desired direction. The electric drivers most commonly used are either stepping motors or dc-encoded motors. Stepping motors take a single discrete step for each voltage pulse received. This step-by-step motion can be easily computer controlled. Readout of the workpiece position is obtained by counting the drive pulses. The dc-encoded motors employ linear or synchronous motors and typically some sort of optical encoding scheme for highly accurate position readout.

Once workpiece positioning is established, alignment must be determined and calibrated (which means finding the correct workpiece position and orientation). Alignment can be a simple or complex process, depending upon the simplicity or complexity of the part to be processed. For a flat, square workpiece, alignment can entail no more than location of one corner of the square to serve as a reference point. This task can be accomplished by physically placing the part in the aligned position and calibrating the motion system. Alternatively, automated visual inspection and location can be used. For this technique, simple image recognition methods are employed to locate alignment marks purposely placed on the workpiece surface. The part is moved until the alignment marks are collocated with reference positions previously coded into the memory of the alignment system.

Automated visual systems for alignment often perform the secondary function of focusing the part with respect to the BDS. There are many kinds of auto-focus systems that have been described in the literature. A common one is based upon the Foucault "knife-edge" technique.[54] In this technique, a collimated input beam comes to a focus on the surface to be processed, and a reflected beam returns on the same path. A beam splitter sends some fraction of the return beam toward a secondary lens, which causes the return beam to pass through a focal point prior to impinging upon a split photodetector operating in a differential mode. As the beam diverges from the secondary focal region, it uniformly fills both sides of the split detector so that the difference is zero and no error signal is generated. At the secondary lens focal point, a knife or razor edge is placed perpendicular to the beam direction, and is then precisely positioned so that the edge just cuts the focal spot and diminishes the light incident upon the split detector. When the part is in

focus, the secondary focal spot coincides with the knife edge, and light remains uniformly split between both detector halves. However, if the part becomes either positively or negatively out of focus, the position of the secondary focal spot falls, either before or after the knife edge, causing more light to fall on one side of the split detector. An error signal proportional to the magnitude of the change in focus is generated and used to make a closed-loop servo system.

There are also diverse manual focusing methods that may serve well in a given situation. Often, the focusing or imaging lens system is an integral part of a microscope system that can be used for visual monitoring of the processed surface. The microscope can then be used to permit visual focusing of the part. Excimer laser systems present some challenges for focusing with microscopes, because the UV radiation of the excimer does not correspond to the visible light the user employs for sight. A surface that appears to be in focus to the eye may, in fact, be out of focus at the excimer wavelength of interest. One solution to this problem is to place a surface that fluoresces visible light under UV irradiation in the same plane as the part to be processed.[55] Irradiating this "quantum converter" surface with very low-intensity, high-pulse repetition rate excimer light induces a visible glow from the surface, which can then be used for precise focusing.

As with all focusing methods, the depth of processing must not exceed either the depth of focus of the lens, or the range over which the lens can move to remain in focus. As the spot of the image size is made smaller, this requirement becomes more of a constraint on the system.

5.4.3 Process Diagnostics

Lasers have a unique advantage over most material processing tools: they can also be used as *in situ* process diagnostics detectors. Beyond the ability for accurately measuring the distance to a surface, lasers have been used to monitor surface deflection, surface temperature, and surface contamination level. Lasers can also be used to monitor the ablation or deposition product species, either in particle form, using Mie or Rayleigh scattering techniques, or as atomic or molecular species, using spectroscopic assignment. In addition, lasers can be used to monitor the surface corrugation and topology, either by scattering or by a time-resolved high-gain optical imaging technique. In this latter technique, the pulsed laser is used to briefly illuminate the surface, and the resultant illuminated image is amplified manifold in a laser gain media. The optical properties of a thin-film deposition process can also be measured by monitoring the change in the laser electric field polarization vector upon reflection. Similarly, the development and subsequent shifting of interference fringes in a reflected beam can be used to monitor the film thickness. A laser can be used to monitor the supporting apparatus or the feed lines in a material processing station, such as measuring the concentration and flow of a particular reagent or the stability and speed of a moving workpiece.

5.5 Utility and Limitations of Laser Processing

A common, but now dated, cliché is that the laser is a solution in search of a problem. While this cliché may have been true at one time, the rapid development of laser science and technology over the past 10–15 years has led to the widespread use of lasers. In materials science, chemistry, physics, environmental analysis, medicine, biology, seismology, and engineering, the laser has developed into a virtually indispensable tool. Similarly, commercial and industrial laser development has resulted in significant military and industrial laser use: range finding, biological agent detection, guidance, packaging structures for semiconductor logic and memory chips, automotive welding, magnetic disk fabrication, video disk mastering, and many forms of drilling and cutting. There are many potential applications for the laser, which are limited only by the creative insight of the technologists involved in this work. Nevertheless, a laser solution may not be optimum for

a given situation, and attempting to force-fit the laser into a particular military, commercial, or industrial setting may be likened to forcing the proverbial square peg into a round hole. A discussion follows of the conditions that are appropriate or not appropriate for the use of a laser.

It should come as no surprise that in the majority of nonmilitary industrial settings, cost/benefit considerations almost always determine the suitability of laser processing. For military ventures, the superiority or unique quality of a product fabricated or made possible by a laser technique is often given high consideration. So, just when is laser processing an acceptable technique for a microengineering application? The many answers to this question can be distilled, as follows:

- When the laser provides a unique and desirable attribute or quality to a part or process that can be obtained by no other technique
- When the laser provides for unequaled reliability in a finished part
- When the laser process permits significantly increased throughput and efficiency, resulting in superior cost effectiveness and a high benefit-to-cost ratio
- When the laser can provide the lowest cost solution, based on many factors, to a fabrication problem

It is often a combination of these answers that justifies the use of laser processing. First, lasers can, and do, perform amazing functions that routinely tip the scales in favor of their use. Often, other techniques and procedures are hard pressed to perform the same functions. If such a function is required for a given application, then a laser should rightly be chosen. Second, laser processing should be chosen if the finished part is to possess high reliability or smooth functioning. This is particularly true if the part is to be used in remote or inaccessible environments that would make replacement or maintenance difficult or impossible. Satellite-borne instrumentation or components are clearly one of these categories where high reliability is paramount. Chemical sensors and associated electronics situated in hazardous environments are another category. Industrial and military users pay for high reliability, and if a laser process can provide that degree of security, then a laser is more likely to be employed. Third, a characteristic of lasers that may result in their use is the potential for high throughput. Often, the speed of laser microprocessing distinguishes it from other methods and techniques. Lasers with large-area beams and/or very high pulse repetition rates possess inherent capabilities for rapid processing. Even if the quality of a processed part or surface obtained through laser and nonlaser methods is similar, a laser technique with a high throughput will win out over a nonlaser method. Simple economics and cost effectiveness dictates that this will be so. Fourth, laser processing should be used if it can produce a given part with sufficient quality and reliability and is also the low-cost solution. The reader may wonder how an expensive laser could ever be the low-cost solution. However, looking at the isolated cost of a laser does not often present a clear picture of the overall cost. Because a laser technique may impart special desirable characteristics while providing for high reliability/repeatability and high production rates, it may often provide the lowest overall cost.

As prevalent as lasers are, they clearly are not used in all situations, nor should they be. Many situations exist where the use of lasers for material processing is not optimum. Even though a laser might provide a processed part of high quality, another simpler, less exotic technique may provide a slightly lower quality part that nonetheless is "good enough." This is an important point that cannot be overemphasized. High quality alone will not always justify the use of a laser technique. The laser's high quality must be coupled with an ability to fill a niche or special requirement that cannot be filled by another method. For example, consider laser wire stripping (to be discussed later in this chapter). Without a doubt, excimer laser wire stripping is of superior quality to CO_2 laser-based stripping. However, many companies use CO_2 stripping because it costs less and is of acceptable quality for the particular application.

5.6 Microengineering Applications

5.6.1 Overview

As a general technology, microengineering has enormous applications in both current and future aerospace systems because it purports to offer functionality at a reduced size and volume. Both of these reductions are valuable benefits to an aerospace system design engineer, whose nominal task is to show functional value for every unit mass to be sent aloft. Aerospace systems—whether for aeronautical or space applications—rely on "engineered" materials and structures to withstand the environment at takeoff/launch, high-speed cruise/ascent-to-orbit, and landing/deorbit and reentry. The requirements for operation can be severe and may impose a wide variation of operational tolerances in temperature (~100 to ~400 K), pressure (1 to $\sim 10^{-13}$ atm), mechanical loading (0 to ~10 g), and radiation flux (0.3 rad/yr to 10^6 rad/yr). Because of these requirements, and similar to some terrestrial applications, aerospace systems manufacturing relies on "clean" material processing techniques and employs a higher level of precision/tolerances than most other manufacturing domains. In this regard, laser-based material processing offers a capability for developing and processing engineered materials with high precision and without physical contact.

The vast number of aerospace applications for microengineering requires the fabrication of precision microholes and cuts in numerous materials, the precise fusion of "dissimilar" materials, and the controlled deposition and adhesion of an overlayer material. A closely related, but somewhat new application, is surface texturing to imbue a material with new characteristics. Finally, a major application is the development of microengineered components/devices that contain onboard "intelligence."

Precision microholes are used in the development of acoustic suppression systems within jet-engine cowlings, in the controlled metering of fluids, and in the development of fuel-efficient micropropulsion systems for future micro/nanosatellite applications. Precise fusion of dissimilar materials is used in the development of functionally gradient materials, such as for thermal control and for developing integrated component packaging. Controlled deposition of novel materials is used in the growth of optically selective films; in the deposition of specialized films for tribology (e.g., dry lubricants for space applications); and in the deposition of thick coatings for protection against the environment. Surface texturing applications include the removal of oxides from metals prior to additional processing and the ruling of fine lines in large array (m^2) polysilicon solar cells. Finally, there are also applications of laser processing to components/devices/microsystems, which are fabricated using semiconductor materials and employ integrated circuit (IC) processing techniques. For these applications, the laser-based processing techniques are used in the high-value-added processing steps, such as for via hole patterning in multichip-module (MCM) packaging, for IC circuit/device trimming/turning, or for rapid prototyping or repair operations. As a further example of high-value-added processing capable only by laser, consider the mundane application of drilling holes. Experiments show that controlling the hole shape (e.g., noncircular) and taper (e.g., noncylindrical) can result in beneficial properties for fluid and acoustic dynamics. This is also true for cutting trenches/lines. Experiments show that trenches/lines cut with noncylindrical shapes or those having rounded bottoms are less likely to fail due to stress concentration. The use of smooth tapers and minimizing the number of sharp corners is considered a viable solution.

5.6.2 3D Microfabrication

Much has been written about direct-write laser micromachining via ablative and chemical assist techniques.[56] These techniques essentially employ a 2D mass removal process with sequential rastering to fabricate true 3D objects. It is also possible to imprint a 3D pattern directly into a

material without laser rastering. This imprinting can be done in a photosensitive material that absorbs at the laser wavelength. By controlling the laser dose and using direct-write patterning, a true 3D image can be imprinted in the exposed volume of the material.[12] There are numerous materials that have these photosensitive characteristics, including certain glass/ceramic materials that also have technological applications to Aerospace systems. In particular, lithium-aluminosilicate glass is a material with ingredients that enable a photographic image to be transferred to the glass after UV exposure and subsequent heat treatment. The latent image is captured by a devitrification process in the glass. There are over 5000 compositions of this type of glass, some of which go by the trade names of Fotoceram, Pyroceram, Photsitalls, Vitrokeram, and Foturan.[57] For Foturan (manufactured by Schott Glassworks, Mainz, Germany), whose photosensitive characteristics arise from the additions of Ce_2O_3 and Ag_2O, photoexcitation and devitrification proceeds as follows. In the unexposed glass state, both the cerium (Ce) and the silver (Ag) are stabilized as ions (Ce^{3+}, Ag^{+}). Upon UV illumination within the material absorption band (Fig. 5.4),

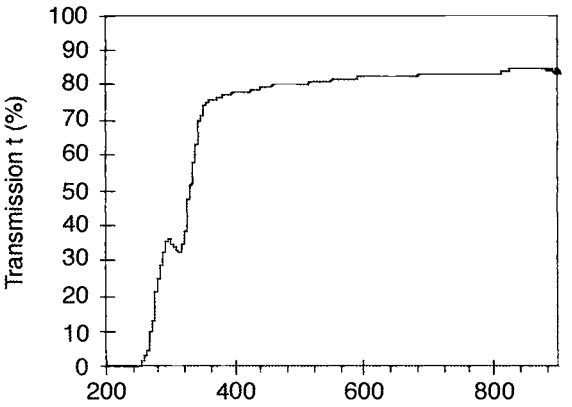

Fig. 5.4. Transmission curve of Foturan, per manufacturer's data for a 1-mm-thick sample.

there is an electron transfer process that neutralizes the Ag^{+} (reaction is shown in Eq. 5.23) and stores the latent image. The ceramization or baking step aggregates the silver nuclei and forms silver-lithium silicates (Eq. 5.24). Upon exposure to hydrofluoric acid, the silicates etch faster than the unexposed glass (Eq. 5.25). Figure 5.5 and 5.6 present data, measured at The Aerospace Corporation (Aerospace), which show an etch rate difference approaching 20:1.

$$\text{Illumination: } Ce^{3+} + Ag^{+} >> Ce^{4+} + Ag^{o} \tag{5.23}$$

$$\text{Ceramization: } nAg^{o} >> (Ag^{o})_n - Li_2SiO_3 \tag{5.24}$$

$$\text{Isotropic Etching: } Li_2SiO_3 + 3HF >> 2LiF + H_2SiF_6 + 3H_2O \tag{5.25}$$

Using the above photoexcitation process, along with some detailed understanding of the nonlinear fluence dependence properties of the material, Aerospace developed a true 3D direct-write laser micromachining technique. The technique uses a focused pulsed UV laser to expose a precise volume of the material. Under computer XYZ motion control, a pattern is "written" in the photosensitive glass. There is no application of resist material, and in general, the exposed volume has a depth dimension on the order of the confocal parameter b. Equation 5.3 can give a general idea of how large a part can be fabricated with this technique. Setting ω_o between 0.5 and 5 μm and λ between 0.2 and 0.3 μm gives a range in the confocal parameter, b, between 5 and 800 μm.

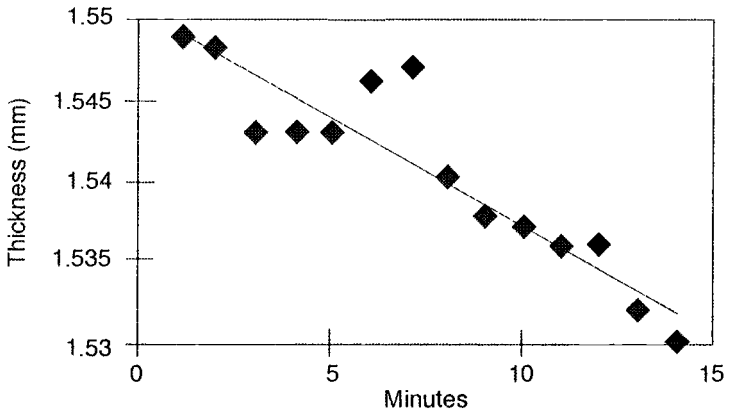

Fig. 5.5. Etch depth as a function of time for an unexposed Foturan sample. Sample was exposed to the ceramization program bake. The linear fit gives an etch rate of 1.3 μm/min.[12] Foturan unexposed—etch depth. $y = -0.0013x + 1.5504$; $R^2 = 0.846$.

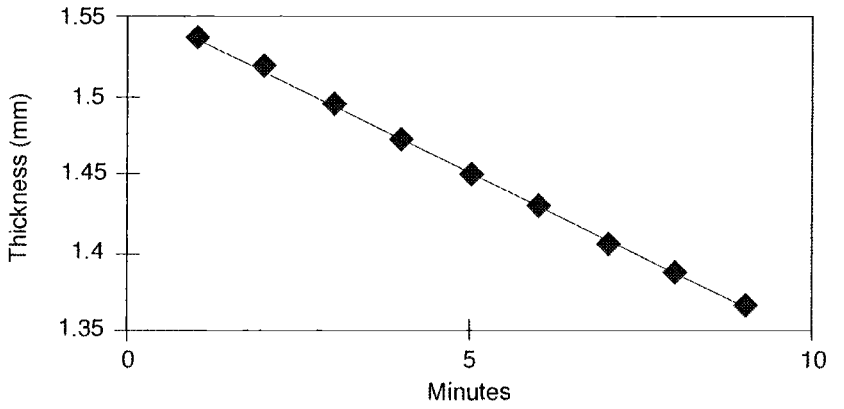

Fig. 5.6. Etch depth as a function of time following 248-nm laser irradiation at 200 Hz and 1.8-mW average power. The linear fit gives an etch rate of 21.6 μm/min.[12] Exposed Foturan—etch depth. $y = -0.0216x + 1.5591$; $R^2 = 0.9995$.

Key aspects of the process are the laser wavelength, the energy dose deposited, and the single shot fluence (J/cm^2). The laser wavelength influences the absorption depth, the total energy dose applied influences the HF etching rate, and the single-shot laser fluence defines the damage threshold. Curved 3D structures can be fabricated by also controlling the spatial contour of the laser beam near its focus. Experiments were conducted using two laser wavelengths (248 and 355 nm). Mesoscale devices were fabricated ranging from 400 to 1500 μm thick with microscale structure in the range of 10 μm. Figure 5.7 shows an optical microscope photograph of two resonant beam structures. Figures 5.8 and 5.9 show scanning electron micrographs (SEMs) of spire structures fabricated by programmed scanning of the X-Y positioning stages with a focused 248-nm laser beam, where the focal spot size is at a constant depth beneath the surface (no Z motion). Figure 5.8 shows an array of pyramidal tips formed by overlapping X and Y scans. The two SEMs show

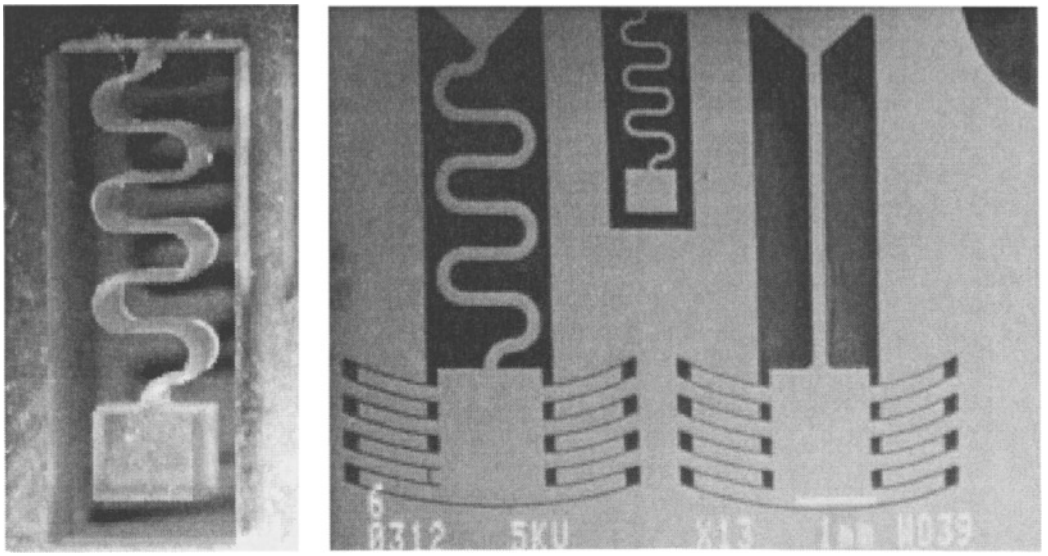

Fig. 5.7. Optical microscope photograph of a resonant beam structure: (left) the structure is approximately 5 mm long and 1 mm deep; the spring meander is 20–40 μm wide; (right) resonant structures with patterned gold.

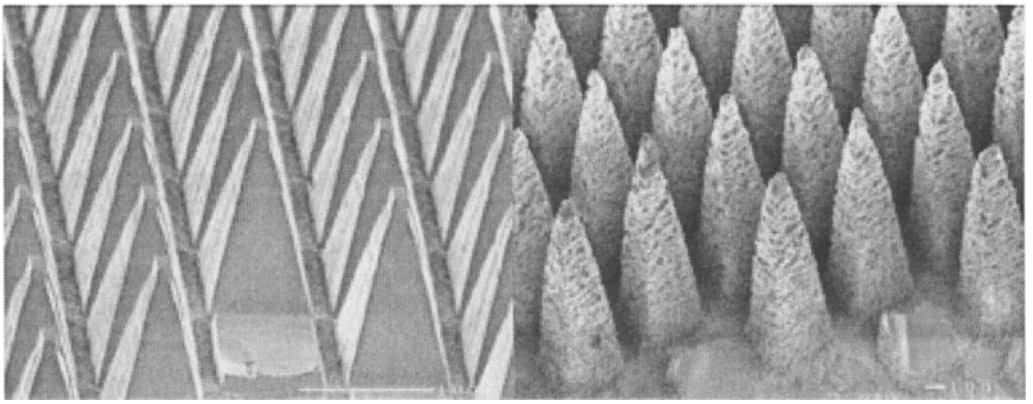

Fig. 5.8. Two SEMs of arrays of spires. The spires are ~300 μm high. By controlling the ceramization step, the spires can be made to have smooth walls or a scaly texture.

microstructures with sharp and rounded corners. Figure 5.9 also shows two SEMs: a series of concentric rings with a central spire formed by coordinated X-Y motion with nonuniform velocity, and a series of rings about a single spire that share a common tangent (1.2 mm maximum diameter by 0.3 mm deep).

The micromachining of "glasses" and ceramics by direct-write techniques enables these materials to be used for other applications besides those in future space systems. For example, these materials can be used in biological applications where glass is preferred over plastics. The applications become especially intriguing if silicon can be directly fused to these aluminosilicate "glasses" via a low-bulk temperature process. Aerospace is investigating the use of laser-based direct-write techniques for silicon-"glass" fusion. The successful development of these

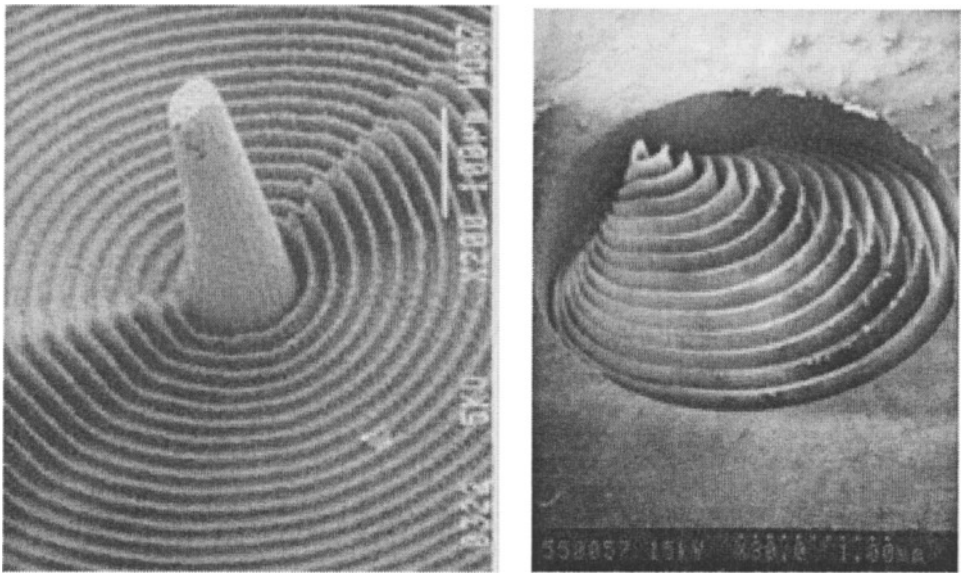

Fig. 5.9. Two SEMs of mesoscale structures fabricated in glass/ceramic material. The left SEM center spire is ~250 μm high, but thin walls are approximately 10 μm thick. The total structure is similar in dimension to the right SEM photo (~2.0 mm). In the right photo, a single spire tip is surrounded by a series of walls, where each wall is of variable height.

techniques will permit the integration of electronics, MEMS, and MOEMS (Microoptoelectromechanical systems) as fabricated in conventional silicon-based foundries with microstructures/devices fabricated in glasses/ceramics. Glass ceramic devices will be especially useful in aerospace applications where caustic propellants that can etch silicon must be used (e.g., hydrazines).

5.6.3 Laser Via Production for MCMs

In 1991, IBM introduced the first commercial mainframe computer that incorporated laser ablation technology in the manufacturing.[58] This milestone was the culmination of nearly a decade of scientific, engineering, and manufacturing effort. Extensive research and development (R&D) on 308-nm laser ablation of a polyimide dielectric resulted in the first IBM prototype ablation tool in 1987 for the production of via holes in thin-film packaging structures. This prototype, similar to a step-and-repeat photolithography exposure tool, evolved into a full-scale manufacturing tool that currently uses sophisticated beam shaping, beam homogenizing, and projection optics.

In 1982, Srinivasan and co-workers discovered the spontaneous removal of material from the surfaces of organic polymers subjected to 193-nm pulsed excimer laser radiation. This discovery led to much scientific interest in this process.[59] IBM was interested because a new method was now available for creating via holes in polymer dielectrics, and this method promised high processing speed and reduced costs. In the early 1980s before this discovery, when thin-film processes for MCM fabrication were being defined, wet etch was the only available low-cost via formation technique. Therefore, the 1983 announcement that polyimide undergoes ablation by 308-nm excimer laser radiation significantly changed the situation.[60] A process using this wavelength meant that optical problems associated with lenses and mirrors at 193 nm would be greatly reduced with operation at 308 nm. Additionally, and perhaps more important, the new 308-nm xenon chloride (XeCl) laser was of higher quality and reliability than the previously used 193-nm argon fluoride (ArF) laser.

IBM exploited the new process by launching an engineering program to develop a 308-nm ablation tool for via formation in MCMs. A chief concern was whether a commercial laser of sufficient quality for a manufacturing environment was available. The common research-type excimer lasers of those years were unsuitable for manufacturing. The component lifetime of the lasers was short, and the output power degraded far too quickly. New lasers offered by several companies, and designed with industrial use in mind, helped to resolve the problem and enable a prototype tool to be built. Further engineering decisions regarding image projection strategy, beam uniformity, projection mask technology, and beam delivery optics culminated in the first prototype ablation tool in early 1987. Much of this early work has been documented by Lankard and Wolbold.[61]

Figure 5.10 displays a schematic of a cross section of the thin-film packaging structure used in the MCMs of the IBM ES9000 computer.[62] Clearly shown are the tapered vias created in the polyimide interlevel dielectric. IBM has explored four different technologies for via production: wet etching, laser ablation, reactive ion etching (RIE), and conventional lithography using photosensitive polyimide (PSPI). Laser ablation has been shown to have fewer processing steps than the other technologies and provides higher throughput in terms of finished substrates per hour. Additionally, ablation is the only fully dry process, allowing additional cost savings. Wet etch, RIE, and PSPI are all highly process intensive, and thus expensive, relative to laser ablation.

The via production process, as currently practiced at IBM, involves four steps: application of the polymer to the substrate, curing, via hole formation by ablation, and final plasma treatment for laser-generated debris removal. The via ablation step is done by projecting the image of a laser-illuminated mask onto a polymer-laden substrate. As with modern photolithography, exposure of the polymer occurs in a step-and-repeat mode, with one chip site on the MCM being ablated in each step. Many stepping actions are required to cover the entire substrate. The details of the optics and BDS have been extensively described in the literature[63] and will be briefly reviewed here (see Fig. 5.2). Pulsed radiation from a commercial industrial excimer laser operating at 308 nm is passed through beam-shaping optics prior to impinging on a beam homogenizer. This "fly's eye" type homogenizer produces a beam uniformity that varies by no more than 3% at the

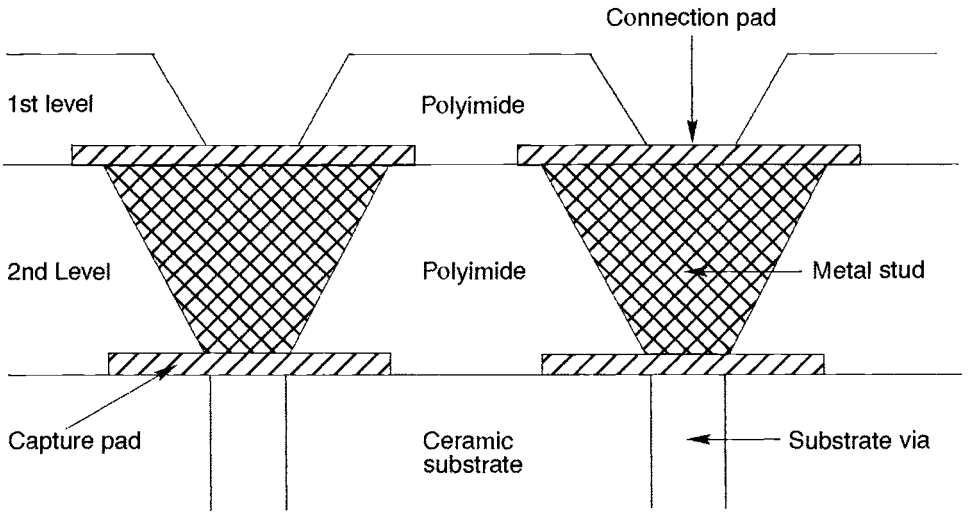

Fig. 5.10. Cross section of a thin-film packaging structure.

substrate image plane. This uniformity is achieved with only a 5% energy loss in transmission. A field lens images the homogenizer output onto a dielectric mask that contains the pattern of vias to be processed. In turn, the mask is imaged by a high-quality, UV-compatible 1:1 transfer lens onto the substrate. The positioning and alignment of the substrate, and focusing of the imaging system, are all under computer control. Figure 5.11 displays an electron microscope photograph of a laser-processed via hole in polyimide surrounded by an ablated pattern of lines and spaces of micron-sized dimensions. A higher resolution view of the lines and spaces is shown on the right of Figure 5.11.

In this via hole production application, ablation is used to generate approximately 10^5 vias on a single polymer level of the substrate. The vias are 75 μm in diameter, and are created in 18 to 20 μm thick polyimide. The two critical parameters for the laser ablation process are the laser fluence and the number of pulses per via site. Both of these parameters can be well controlled, but in practice, tight control is not necessary. Variations in laser fluence of up to 5% are acceptable because many pulses are required to completely form the via and any variation is averaged out. Depending on the particular substrate and process, a laser fluence in the range of 150 to 300 mJ/cm^2/pulse is employed. The number of laser pulses needed for a given polymer thickness is determined from standard ablation rate curves. At an ablation rate of 0.1 μm/pulse, a 20-μm-thick polymer sample would require about 200 pulses to completely form the via. At 200 pulses per second from the laser, via hole formation would take approximately 1 s. A suitable number of excess pulses are used to ensure that all vias are completely formed, and that small variations in polymer thickness and pulse-to-pulse fluence do not adversely affect the result. Since nonerodable metal pads reside at the via bottom, these excess pulses cause no further ablation at the fluences employed.

As can be partially seen in Fig. 5.11, the via wall angle is less than 90 deg. This angle results from the inability of the lens system to transfer high-contrast images from the mask to the polymer surface. Additionally, the high intrinsic absorption of the polyimide further inhibits perfect fidelity of image transfer. This wall angle turns out to be quite useful in increasing the adherence of metal that is subsequently deposited into the via hole. The via wall angle can be controlled very tightly between about 40 and 70 deg by changing the focal plane for ablation.[64]

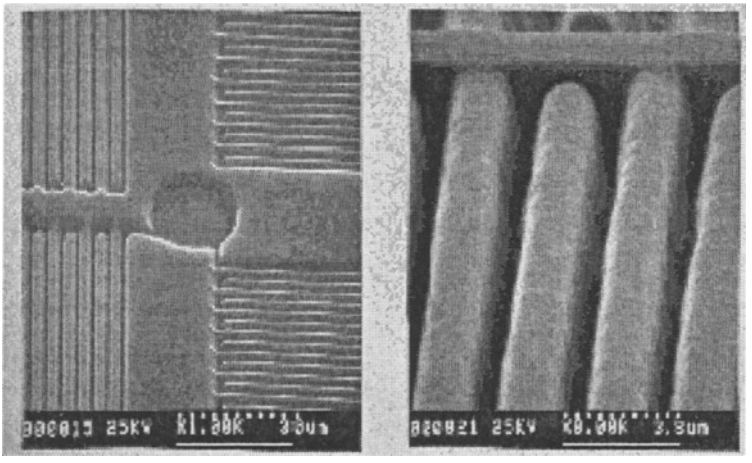

Fig. 5.11. SEM photos of polyimide via hole (left) with micron-sized lines and spaces (right). The scale bar on the left hand SEM is 30 μm; the bar on the right is 38 μm.

IBM's early laser-projection tools for via fabrication were to a large extent designed and built in house. While the tools served the needs and demands occurring from 1985 to 1987, such as low-volume production rates and flexibility, they were woefully inadequate for high-volume manufacturing. As a result, continual improvements were made in the tools. Table 5.5 gives a profile of the major tool improvements between 1987 and 1994. While not explicitly stated in the table, improvements in the beam-delivery optics, the laser, and the computer automation drove most of the advances. For example, improvements in the fabrication and assembly of the imaging lenses allowed significantly smaller vias to be created. Likewise, longer gas lifetimes, increased reliability in high-voltage components, and advanced discharge electrodes all greatly improved

Table 5.5. Improvements in the Laser Via Process

Parameter	1987	1994
Process cycle time	25 min	12 min
Via wall-angle range	50–65 deg	20–75 deg
Minimum via size	11 μm	6 μm
Exposure field size	14×6 mm^2	40×30 mm^2
Substrate alignment	Manual	Automated
Alignment accuracy	±7 μm	±1 μm
Tool availability	50%	>95%
Process yield	~ 85%	>99.99%

the laser. This improvement resulted in vastly improved tool availability, defined as the percent of time the tool is operational relative to the demand time. Computer-controlled alignment and focusing reduced the errors in substrate positioning to the micron level. As a result of these many improvements, the mean-time-between-failure (MTBF) for the ablation system grew from about 150 h to over 700 h for the current system. The MTBF for the laser itself went from a few hundred hours to well over 1000 h–a significant measure of success. The demand time for the via fabrication tool is approximately 150 h/week.

The laser process for via hole fabrication has been used at IBM for nearly a decade. During this time, several billion vias have been produced in a variety of thin-film packages, including MCMs. There have been no known field failures of vias. Clearly, this is one of the most robust, reliable, and high-yield technologies in the thin-film fabrication industry.

IBM chose the laser technology for via hole creation because it could provide highly precise and defined vias, high-speed parallel processing that was compatible with large-volume manufacturing, an environmentally sound dry process, higher than acceptable reliability, and the most cost-effective manufacturing solution.

5.6.4 Laser Wire Stripping

Advanced techniques for localized removal of plastic insulation have found significant application in microelectronic packaging and interconnect technologies. One such application is the laser via process described in the preceding subsection. Another application is the removal of the plastic insulation that typically covers electrically conducting wires. This wire stripping has been

performed by a variety of techniques in the aerospace, data storage, and electrical industries. Techniques include mechanical cutting, abrasive action, electrical arcing, chemical etching, and simple thermal methods such as burning. These thermo-chemical-mechanical techniques can be used, and often are, when the wire is of sufficient durability, and when the processing speed, precision, or cleanliness of the stripped region is of no great concern. However, for many applications in the microelectronic and computer industries, strip length, precision, and cleanliness are major concerns and thus significantly restrict the available choices for wire stripping.

In the magnetic disk drive industry, a small read/write head is part of a ceramic slider that is suspended above a spinning disk. Electrical signals are conveyed to and from the head by very fine magnet wires (20–50 μm diam) that connect to the supporting electronics. These wires must be bonded to the head in such a manner that electrical contact is made. Adequate bonding only occurs if metal-to-metal contact is made between the magnet wire and the bonding pad on the slider. This contact is accomplished by the removal of the polyurethane-based plastic insulation in the vicinity of the region to be bonded. The conventional industry technique for wire stripping has been the use of electrical arcing. While this has been an inexpensive and efficient method, it lacks the cleanliness, and particularly the strip location precision, necessary for current and future generations of head suspension systems. Imprecision in the strip length or location may result in electrical short failures. To resolve this problem, the magnetic drive industry is exploring the use of laser wire stripping.

Laser-based methods for wire stripping, usually employing pulsed or cw CO_2 lasers, have been used in many industries since the mid-1970s.[65] Laser wire stripping offers the advantage of being a noncontact method–a significant factor for the small, precision parts currently used in microelectronics. Another advantage is that light can be imaged to small, divergence-limited spot sizes, allowing very small lengths of insulation to be stripped. For example, using the UV wavelengths of an excimer laser, a strip length as short as 10 μm should be possible. However, the light absorption properties of the insulation are much more important for effective wire stripping than are the imaging capabilities of the laser wavelength employed. As will be discussed, precision laser wire stripping requires the plastic insulation to absorb the laser radiation very strongly, and requires the laser energy to be delivered in pulses short enough to limit thermal diffusion effects.

Primarily because of its high power and relatively low cost, the CO_2 laser has been used in many wire-stripping applications. The laser emits IR radiation peaked near the 10.6-μm wavelength–a spectral region where most plastic insulations absorb only moderately. Typical absorption coefficients for plastic films are in the range of 10^2 to 10^3 cm^{-1} for CO_2 radiation. Because of this limited absorption, wire stripping with the CO_2 laser requires that the light be focused for sufficient intensity to break down the insulation. Further, the moderate absorption can limit the efficiency with which the last few insulation layers are removed, resulting in thin nonconducting layers remaining on the wire. To prevent charring of the edge in the stripped region, the CO_2 laser is often run in a gain-switched pulse mode. Focusing of the pulse onto the insulation surface initiates dielectric breakdown and rapid ejection of molten and solid material. Stripping of the localized wire region can be accomplished in just 2 or 3 pulses incident from a few circumferential directions. The strip edge definition is not optimum, and debris generation can be problematic. Nevertheless, in many instances, this edge definition is of acceptable quality. When exposed, the high reflectivity of the bare (stripped) wire to CO_2 radiation protects the metal from unacceptable levels of heating and consequent mechanical fatigue.

In addition to the CO_2 laser, the excimer laser is used in many wire-stripping applications. Specifically, for high-precision, efficient removal of wire insulation, the excimer laser is the laser of choice for several reasons.[66] One reason is that most plastic insulators strongly absorb UV light.

The short (10–20 ns) pulse of the excimer laser, along with the deep UV output, provides a strong absorption event in a very short time. It is almost ideal for wire-stripping applications. As the pulsed excimer radiation interacts with the plastic insulation, the light only penetrates a short distance. For polyurethane insulation, the measured absorption coefficient at 248-nm wavelength is about 7×10^4 cm^{-1}, providing a short penetration depth of less than 150 nm. The deposited energy is some 2–3 orders of magnitude larger than that for the CO_2 laser. At the 308-nm excimer laser wavelength, the absorption coefficient is less than 3000 cm^{-1}, accounting for why this wavelength provides stripping action considerably less appealing than the 248 nm wavelength. Regardless, the absorption coefficient is larger in the UV than the IR, which results in a number of advantages that makes the excimer technique the better choice. For example,

- In the UV, the shallow penetration depth causes only a thin layer to be ablated per pulse, with the result that many pulses are required to completely strip a wire containing a 5-μm thickness of insulation. This approach to material removal promotes control and aids in defining the edge with precision.
- Strong absorption in the UV aids in the removal of the last residual layers of insulation, helping to provide clean surfaces.
- Strong absorption means that the laser light decomposes the organic matter, which significantly reduces debris.
- Strong absorption means that the laser beam does not have to be focused on the surface; rather, the incident laser intensity can just be above some threshold value for insulation removal.
- Strong absorption means that blocks of insulation can be removed by image projection rather than by scanning a focused laser beam. The result is increased efficiency and high throughput.
- UV laser short pulse limits thermal diffusion and heating of the wire in the laser irradiated region, thereby aiding edge definition and precision.

Figure 5.12 displays an optical configuration for performing excimer laser wire stripping. Pulsed 248-nm radiation illuminates a mask. The mask is imaged by a single lens onto the plane where the wire is vertically held. The image size at the wire plane is controlled by the size of the mask and the imaging system. The image height determines the wire strip length. Because the width of the image is much greater than the wire diameter, most of the light passes by the wire

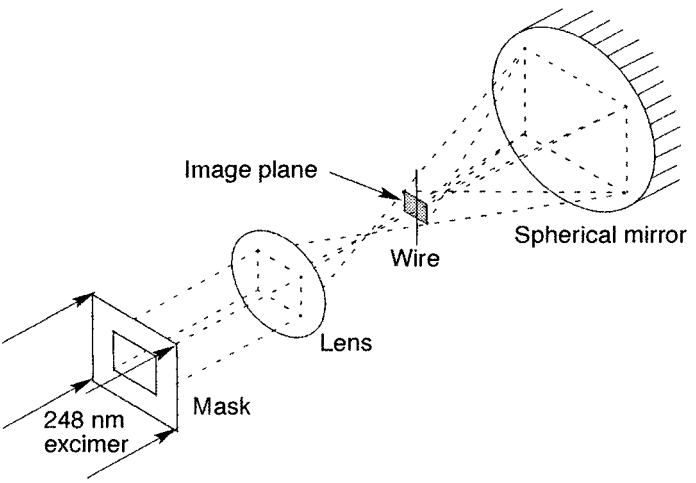

Fig. 5.12. Optical schematic for excimer laser wire stripping.

and is intercepted by the spherical mirror. At the mirror, the radiation is reflected and reimaged onto the back side of the wire for insulation removal. In this manner, excimer pulses strip the entire 360-deg circumference in a single-beam configuration, without resorting to multiple beams or rotating wires.

Excimer laser wire stripping is performed on polyurethane-based insulation using incident fluences of 300 to 400 mJ/cm^2/pulse. Approximately 100 pulses are required, and can be accomplished in less than 1 s using high-pulse repetition rates. Figure 5.13 shows electron microscope photographs of an excimer-laser-stripped magnet wire. The stripping is clean and well defined, with no evidence of debris.

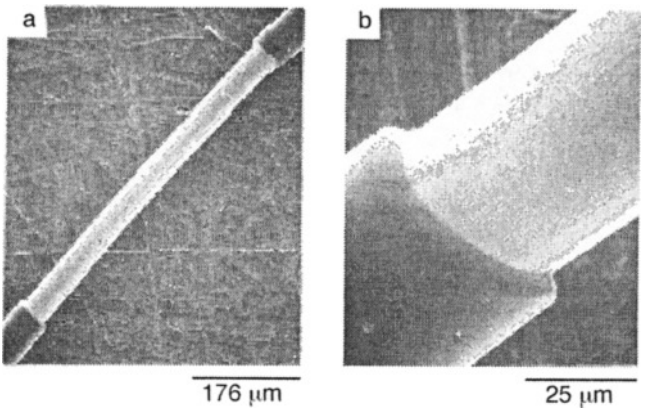

Fig. 5.13. SEM photographs of 248-nm stripping of magnet wire.

One drawback of the excimer laser is the expense required to operate and maintain this device. This is the reason why CO_2 lasers, although not as precise, are often considered "good enough" for the application. Furthermore, once the metal surface is exposed, excessive excimer intensity may cause heating effects that can prove deleterious to the mechanical strength of the wire. These effects are much more of an issue with excimer lasers than with CO_2 lasers, because UV radiation is more strongly absorbed by metals than is IR radiation. For this reason, the number of excimer laser pulses and their intensity must be carefully chosen and maintained.

In conclusion, laser stripping of magnet head wire has proven itself as an industry standard technique for a variety of reasons. First, although trade-offs exist in the merits of excimer laser versus CO_2 laser-stripping techniques, laser stripping provides much higher throughput than non-laser stripping techniques. Second, this higher throughput is coupled with high precision in both the length and placement of the stripped region. Third, the noncontact laser process reliably produces a finished part that ultimately costs less than parts stripped by other techniques.

5.6.5 Laser Texturing of Magnetic Disks

The data storage industry has an increasing need for higher storage capacities.[67] One method for increasing capacity is to increase the areal storage density on the disks within a magnetic hard drive. The physics of the magnetic read/write process dictate that a higher areal density can be achieved by having the magnetic head (which contains the read element) fly closer to the rapidly spinning disk. Currently, the magnetic head flies 30–100 nm above the disk. To have the head fly closer to the disk, and thus achieve higher areal storage densities, requires that the disk surface must be smoother and flatter than in the past.

One problem with reducing the surface roughness of a disk is the increased area contact between the disk and the "slider." (The slider is the smooth ceramic element containing the magnetic read and write head, which is suspended above the disk when it is spinning.) The disk/slider contact results in frictional forces that tend to increase wear on both the slider and the disk. In extreme cases, the slider can become stuck to the disk surface. This phenomenon has earned the moniker "stiction" for the sum total of all attractive forces between the smooth slider and the smooth disk. The tribology problem in the magnetic storage industry has been, and continues to be, finding ways of reducing stiction and wear to acceptable and controllable levels.

Because stiction is proportional to the area of contact between a slider and disk, one way to achieve low stiction is to minimize the contact area. For years, the storage industry has minimized the contact area by performing a full-surface mechanical texturing of the disk. Surface texturing alters, in a controllable fashion, the surface topography such that the contact forces between the disk and the slider are reduced in a known manner. This approach has worked for relatively low areal density disks that do not require very low slider flying heights. However, for the current and future generation of hard drives, this is an unacceptable approach because the full surface roughness does not permit the magnetic head to fly close to the disk. Because of this roughness, the industry has pursued disk texturing in a dedicated "landing zone" near the inside diameter of the disk. In this zone, the requirements of slider-disk tribology can be optimized apart from the requirements of the data zone that constitutes the majority of the disk surface. In the landing zone, the slider can be parked and latched after the drive has been shut down.

For texturing of the landing zone, pulsed laser irradiation has been demonstrated to be effective.[68] At high repetition rates, a short pulsed laser creates discrete topographical features that have domelike protrusions, or "bumps." The bumps are sized and spaced such that hundreds of them are present under the slider, serving as smooth support points. Laser zone texture (LZT) provides an efficient, quick, and high-precision texturing method with excellent tribological performance. This method is so successful that it has permeated the entire magnetic storage industry, becoming a standard manufacturing tool.

The technique of LZT is dependent on the type of disk substrate employed. Current-generation disks consist of an aluminum substrate plated with about 10 μm of amorphous nickel phosphorous (NiP) to improve smoothness and hardness. It is this NiP surface that is zone textured using a solid-state neodymium laser. Subsequently, the magnetic layers are deposited upon the textured NiP layer. A carbon wear layer, followed by a thin lubrication layer, completes the thin film disk. Future requirements of disks demand that they be smoother, flatter, harder, and stiffer than aluminum. Glass substrates nicely fit this demand, and are starting to appear in advanced hard drives. Because of its hardness, the glass surface can be directly textured. The differing optical properties of glass in comparison to metal (highly transparent to 1 μm wavelength Nd laser light) require that a pulsed CO_2 laser perform the texture operation, followed by the deposition of magnetic, wear, and lubrication layers.

For NiP texturing, a high-repetition rate, Q-switched Nd:YLF or Nd:YVO_4 diode-pumped solid-state laser is usually employed.[69] This type of laser is chosen for several reasons: (1) the near-1-μm wavelength radiation is strongly absorbed by the NiP, permitting efficient texturing; (2) the short-duration pulse (40–80 ns) creates high-focus intensities that rapidly melt the NiP and initiate the bump-formation process; (3) because one bump is formed per incident laser pulse, the laser's efficient operation at high repetition rates (20–80 kHz) permits rapid texturing and thus high disk-processing rates; (4) the pulse-to-pulse energy stability is excellent (less than 1% variation), resulting in highly uniform texturing.

Glass substrates strongly absorb near a wavelength of 10 μm. Because this absorption coincides with the output of CO_2 lasers, this laser is employed for LZT of glass.[70] Pulse modulation of CO_2 lasers is obtained by either direct modulation of the RF plasma excitation, or by use of an acousto-optic modulator operating on a cw beam. The latter technique permits rapid pulse repetition rates from 10 to 100 kHz. As with the neodymium lasers, the pulse energy variation is low, consistent with the observed uniform texture process. In contrast, however, the practiced modulation methods limit the pulse duration to no less than a few microseconds. This limitation presents no practical constraint because well-formed texture bumps are nonetheless created.

A schematic of the texture apparatus, for either NiP or glass texturing, is shown in Fig. 5.3. The rapidly pulsed laser is shuttered to control the placement of the texture bumps on the disk. The disk is mounted on a rapidly rotating hub, which in turn is translating. At the same moment, the shutter is opened, and a continuous train of pulses passes through a lens and is focused on the disk surface. Each pulse creates one texture bump. After 1 to 2 s of exposure, the shutter closes and terminates the operation. The spinning and translating motion of the disk creates a spiral of texture bumps in a narrow zone that is 2–5 mm wide. The texture zone placement is precise to within 10 to 50 μm.

One of the distinct advantages of LZT is the microtopography of the generated bumps. Because of this microtopography, the top portions of the bumps are extremely smooth and rounded, which aids in their durability and reduced stiction behavior. For NiP or glass texturing, a single focused pulse creates a single bump with a diameter from 5 to 20 μm, depending on LZT conditions. Further, the height of the texture dome ranges from just a few nanometers to several hundred nanometers. These bumps, though different in geometry for NiP and glass (see below), are extremely shallow, with the slope angle on the side being no more than 1 deg. If the correct pulse energy is established, true nanomanipulation of the texture bump heights can be achieved. In essence, micro- and nanotechnology is positively affecting the data storage market through laser topographic modification.

Figure 5.14 displays the so-called sombrero bump that forms on NiP and the smooth microdome that forms on glass surfaces. Qualitatively, the individual bump geometry is different, reflecting the different formation mechanisms for both surfaces. On NiP, the short and intense pulse

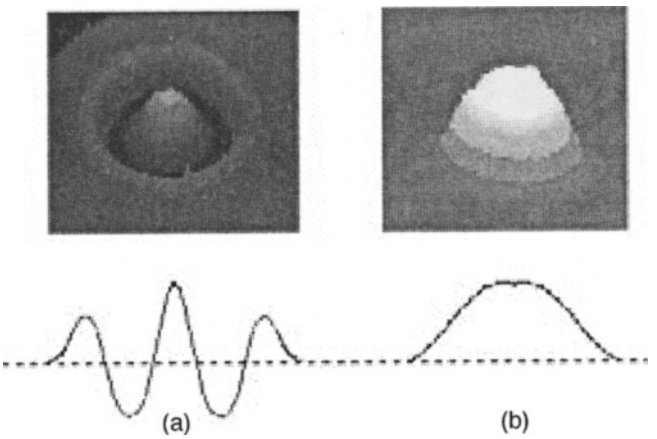

Fig. 5.14. Examples of laser texture bumps. (a) "Sombrero" bump formed by a Nd:YVO_4 laser pulse on a NiP substrate. (b) "Microdome" bump formed by a CO_2 pulse on a glass substrate. Below the photos are typical cross sections of the bumps. (a) sombrero, (b) microdome.

transiently melts the NiP, permitting competing surface tension effects to come into play.[49] The height of the central dome, either above or below the outer rim, can be manipulated by pulse energy adjustment. On glass, the focused CO_2 pulse transiently heats the material to a "softening" point at which material can flow. This flow is induced by normal thermal expansion of the glass and by compressive surface stress that exists because of chemical strengthening of the glass. Because only a small region of material is heated, the main material flow is upward, creating the dome. As with NiP, adjustment of the pulse energy permits variation of the resultant dome height. The NiP melting and the glass softening both create situations where the dome top becomes microscopically smooth. The small laser/substrate contact area and the smoothness of the processed area result in excellent start/stop wear behavior and bump durability.

At a recent 1996 disk industry show, no less than six companies were offering turnkey laser texture tools. In addition, several other companies offer lasers specifically made for disk texturing. Automated laser texture tools (LTTs) for the disk industry offer a high throughput, cassette-based operation. Cassettes of disks are loaded into an input conveyor, and processed cassettes are unloaded from the output conveyor. The procedure is highly controllable, permitting repeated creation of a preselected bump profile. The bump spacing and bump placement are likewise highly controllable. Depending upon the make and model of the automated tool, and the type of processing, process rates extend from 100 to 500 disks per hour.

In conclusion, it is clear that the laser microdome formation process is a success story. The reason for the success of this process, as with all successful laser microengineering techniques, lies in its ability to fill a niche filled by no other process in a cost-effective manner. Although techniques exist for zone texturing by mechanical methods, the zone so produced is of poor quality and has only imprecise placement at best. Similarly, lithographic methods have been used for zone texturing. However, this latter process is relatively expensive and hence not suitable for high-volume manufacturing. The microscopic resolution properties of laser light, coupled with the laser's ability to interact with material surfaces in a unique way, has made the LZT process the solution of choice for the high-end disk drive market.

5.7 A Case Study: Developing a PLD Materials-Processing Tool

5.7.1 Introduction

PLD has become an active area of materials research over the past decade. It is estimated that, to date, over 300 different materials have been deposited using this unique physical vapor deposition (PVD) process. The bulk of the work has focused on various oxide compounds such as high-temperature superconductors (HTSs). However, a significant amount of work has focused on materials that are of potential interest to aerospace engineers, such as wear- or scratch-resistant coatings and tribological coatings.[71] Such materials include diamond-like carbon (DLC), amorphic diamond, cubic boron nitride, and various thin-film lubricants such as WS_4, MoS_2, and TiC.[71] Further research is being conducted on new materials such as C_3N_4 and various other nitrides.

PLD offers many well-known advantages over other PVD techniques, and is therefore an attractive process for materials research. The advantages of PLD can be summarized as follows:

- Ease of stoichiometric transfer of complex target compositions directly to the deposited film
- Ability to deposit films in a wide variety of background gas species
- Ability to conduct ion-, neutral-, or photon-beam-assisted depositions
- Ease of target changes, permitting multilayer film growth

It is difficult to find another PVD process that offers as many features as PLD. When developing a PLD system, certain basic issues must be addressed. The following section focuses on these

issues. The discussion is directed towards aerospace applications but is also relevant to almost all other categories of applications. For the discussion, it is assumed that the reader has some degree of familiarity with the rudimentary aspects of the PLD process. An excellent review of this subject is given by Chrisey and Hubler.[71]

5.7.2 Basics of PLD System

In order to develop a viable PLD tool, the materials scientist must first answer several questions about the nature of the research that is to be conducted. These include the following basic questions.

- What materials or class of materials is to be deposited?
- What substrate materials and shapes will be used?
- What is the substrate size (dictated by the minimum device requirements)?
- What final film thickness will be required for the application?
- What is the maximum temperature the substrates can tolerate? How does this temperature compare to the melting point or crystallization temperature of the material to be deposited?
- Does the material system or device require multilayer film growth?
- What potential background gases will be required for the materials to be deposited?
- Is the process or material of interest sensitive to background gas species such as water vapor?
- Will ion-beam or photon-beam-assisted deposition be necessary to ensure growth of the proper phase?
- What deposition rates and throughput will be necessary for the application?
- What is the available budget for the PLD tool?
- Will the tool be designed and assembled in-house, or purchased as a complete system?

The last two questions should be considered carefully. A typical mistake is to add up the projected costs of all the tool components and then to expect an outside vendor to sell such a system for these costs. Usually ignored in this calculation are thousands of small items (e.g., cables, connectors, water flow switches, power distribution, safety interlocks) as well as the extensive time spent on system design, engineering, and assembly. While design can be conducted "in-house," the cost of design is not typically included in the estimate of a system price. It typically takes about 1 man-yr to properly design, procure, and assemble a working PLD system for a group well versed in deposition and vacuum technology. Therefore, depending on the overall system complexity, a realistic purchase price from a competent vendor is typically two to three times the apparent component "costs." In addition to cost, there are other ancillary issues that should be considered. These issues include the versatility of the tool handling the step that follows PLD in the materials development process, and the question of whether the system should be scaled up to include a larger deposition area, or should branch off into different or more complicated material systems and/or processes. Figure 5.15 shows a schematic of basic large-area PLD system based on a rectangular box design.

When designing a PLD system, the following items should be considered: laser, deposition chamber, substrate heater, target, BDS, pump, deposition rate monitor, and large-area PLD. A discussion of each of these items follows.

5.7.2.1 Laser

In PLD processing, it is strongly recommended that a UV excimer laser be used. Compared to IR or visible lasers, UV lasers generate fewer particulates because of the smaller (~100-nm) absorption depth. In general, higher quality films are grown when UV excimer lasers are used. In addition to the UV output from excimer lasers, the UV output (fourth harmonic) from Nd:YAG (and

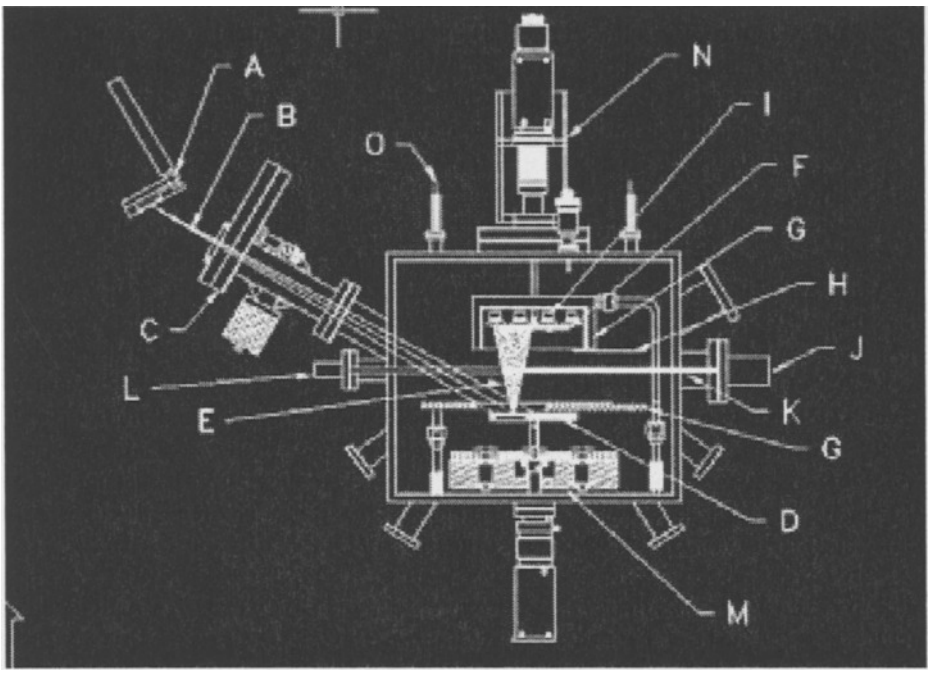

Fig. 5.15. Schematic of a large-area PLD system. A–raster mirror assembly, B–rastered laser radiation, C–Intelligent Window, D–ablation target, E–plume, F–substrate, G–water-cooled shield, H–shutter, I–heat lamp, J–hollow cathode lamp, K–HCL radiation, L–detector, M–target manipulator assembly (only one target shown), N–substrate linear/rotary feedthrough, O–current feedthrough.

other) lasers have also been used in PLD. However, current Nd:YAG lasers produce insufficient UV output powers to obtain reasonable deposition rates over useful substrate sizes. Furthermore, Nd:YAG lasers have a much higher beam quality, which is actually a drawback for PLD. The excellent Gaussian beam profile allows the YAG beam to be focused to a very small spot that yields very high fluences. Energy densities achieved with these lasers can actually melt the target, increasing particle generation tremendously. Expanding the YAG beam to reduce the fluence produces a larger spot with a very nonuniform energy density. The excimer laser, on the other hand, produces a large rectangular output, typically 1 × 2 cm. The energy density over the rectangle is usually uniform (if the laser is working well), except at the edges. Using an appropriate BDS train, the output can be focused down to a spot on the order of a few millimeters square with reasonable uniformity. In summary, excimer lasers offer the best characteristics for the PLD process, because they provide sufficient peak power (~100 MW/cm^2), usable average powers (10–100 W), and multi- or random-mode operation to obtain practical deposition rates and good uniformity. For example, an excimer laser operating at 248 nm (KrF), delivering ~500 mJ per pulse with a repetition rate of about 50 Hz or higher, is more than sufficient for the growth of most materials with reasonable deposition rates (0.5 to ~2 μm/h), over a 2- or 3-in.-diam substrate. Lasers that produce very high pulse energies (~1 J/pulse) are only useful if the ablation threshold for the material is very high. Such lasers rarely operate at the rated output power for an extensive period (irrespective of the vendor claims) and can be very problematic in the long run. Thus, care should be taken in determining the proper size of laser for the application; a 1 J/pulse laser is not necessarily the best choice. Running the laser at lower output is difficult, because the pulse-to-pulse stability is

best when the laser is operated close to the rated output. In high-fluence PLD, most of the incident energy is absorbed in the laser-induced plasma, and the yield of particulate generation tends to increase. High-fluence ablation is typically used for the deposition of DLC films (and usually at 193 nm).[72] High fluence can also be achieved with smaller lasers and the appropriate BDS. However, for several of the materials of interest to aerospace engineers, the deposition rates are typically very low. Materials such as carbon (to form DLC) and carbides used as wear-resistant or protective coatings have very low deposition rates per laser pulse. If these are the materials of interest, a laser with a high repetition rate (~150 Hz or higher) and at least 600 mJ/pulse should be seriously considered in order to obtain reasonable growth rates and throughput.

When purchasing an excimer laser, the user must consider both the physical size of the laser and other additional operational costs. Typical lasers are on the order of 4 to 6 ft long, 3 ft wide, and 2 ft high. Additional costs include the facilities (electrical power, multiple stainless steel gas lines, water cooling, and exhaust vent); supporting table (does not need to have vibration isolation); several high-purity gas regulators; and a cabinet for the halogen gas and high-purity gases. Other ancillary expenses might include an energy detector, a gas purifier, a beam attenuator, safety shields and eyeglasses, and a water chiller (because the higher power lasers and some components in the PLD system may require water cooling). All of this equipment, plus the size of the laser, should be taken into account when procuring the appropriate laboratory space for a PLD system.

In addition to costs just mentioned, there are laser maintenance expenses, which include replacement optics (for the laser and the BDS) and halogen filters. Also, every few years, the internal electrodes and preionization pins must be replaced in the excimer laser. Another issue that impacts cost is the selection of which gas to use in the laser. Argon is significantly less expensive than krypton. However, the reduced amount of energy obtained with argon, and the extra wear and tear on the laser cavity and optics that occurs at the 193-nm (ArF) wavelength, makes krypton (with the laser operating at the 248-nm [KrF] wavelength) a better choice for most PLD applications. As mentioned before, 193 nm is the best wavelength to produce high-quality, optically transparent DLC. If the user plans to use ArF (193 nm) with high repetition rates, then the optical beam path should be purged to remove oxygen. The purging should be done because 193-nm radiation produces ozone in air, which is a serious health hazard. A simple Lucite box purged with nitrogen or argon is sufficient for this purpose and will also keep all of the optics clean.

Excimer lasers also operate at a 308-nm (XeCl) wavelength. The gain at this wavelength is not as high as the gain at 248 nm, but in general the gas lifetime is longer. The 308-nm excimer wavelength is also less punishing to the laser optics but is considered more of an eye safety hazard. Long-term exposure to even low levels of 308-nm scattered light can cause glaucoma. Glaucoma does not occur as readily at 248 nm. However, the 248-nm light can cause an eye condition known as "welder's blindness," which can be treated in 24 h. It is easy to change from ArF (193 nm) to KrF (248 nm) and back again with little downtime. Changing the laser over from a chlorine-based system to an fluorine-based system is not recommended.

Although excimer lasers are valuable for PLD sources, they have only four distinct wavelengths of operation: 351 nm XeF, 308 nm XeCl, 248 nm KrF, and 193 nm ArF. The PLD technique would benefit if the laser wavelength could be altered to match the peak absorbance in the target material. This requires a widely tunable laser with high power. The FEL can be designed to be widely tunable. The Department of Energy (DOE) Jefferson Laboratory FEL is in the commissioning phase to provide tunable kilowatt-pulsed laser power in the IR. The laser is designed to be upgraded to produce tunable laser power in the UV. This facility will provide tremendous insight into the interaction of light with materials. The ability to tune the laser radiation over a

wide spectrum will likely allow the materials scientist to more easily couple the radiation to a specific target material. The strength of the absorption will be strongly dependent on the chemistry (bond nature) of the target. By tuning the laser to individual target chemistry, the user may be able to break specific bonds or to couple energy to the target material in various modes, such as excited electronic or vibrational states. This energy can then be transferred to the growing film, enhancing various film properties such as crystallinity.

Two examples of strong coupling to specific target material as a function of laser wavelength follow. As a first example, the optical quality of DLC films grown from graphite targets is clearly best at 193 nm. The optical quality is best at this wavelength because the more energetic photons obtained with 193-nm radiation break almost all of the carbon-carbon bonds. The result is an energetic plume consisting mostly of individual carbon atoms, with very few dimer molecules.[72] The energetic plume increases the likelihood that sp^3 bonds will form when the carbon condenses at the substrate surface. Films grown with KrF primarily have dimers in the plume, and yield films predominantly made up of the stronger sp^2 bonds. On the other hand, the basic electrical properties of yttrium barium copper oxide (YBCO) (the high-temperature superconducting compound) films are usually very similar, regardless of the laser wavelength used (193 or 248 nm). In this case, the more energetic radiation at 193 nm does not play a significant role (other than a slight reduction in particulates). As a second example, in unpublished work, metallic films made from metal-carbonyl targets were deposited using two different wavelengths. When the target is ablated, it ejects carbonyl compounds that decompose upon impinging on the heated substrate. The volatile carbonyl radicals desorb, leaving a metallic film. Using radiation from 193 nm with fluences of about 1.0 J/cm^2, the film growth rate was on the order of 0.5 μm/h at a 30-Hz pulse rate. Using radiation at 248 nm, just three laser pulses completely covered the entire vacuum chamber walls with several microns of the carbonyl material and covered the hot zone with a thick metallic layer, destroying the substrate heater. While this result was totally unexpected (and the system had to be cleaned and rebuilt, which took several days), it clearly demonstrates that the right combination of target material, coupled with the proper laser wavelength, can increase deposition rates. Also, the right combination can significantly alter the electronic properties of the ablation plume and thus, of the deposited films. While both the excimer and Nd:YAG lasers provide several discrete working wavelengths, they do not offer the capability to continuously vary the wavelength over the wide range that is available with the FEL. Future upgrades of the FEL will include high-power operation in the 190–300-nm range. Another interesting feature of the FEL is its very short pulse length. A short pulse length may significantly reduce the amount of particles that are generated in the PLD process.[71] It is expected that radiation from the FEL will become an active area of research for PLD material scientists in the near future.

5.7.2.2 Deposition Chamber

For the vacuum chamber design, attention should be primarily given to the substrate holder, the substrate heater (if one is required), and the target or targets (if multilayers are required). Several vacuum chamber styles have been used for PLD, including a simple four-way cross, a sphere, and a bell jar, all with extra ports. An alternative design includes a rectangular box chamber with a large hinged access door and several ports. Figure 5.15 shows a schematic of a rectangular box chamber design. Every chamber should be designed around the largest substrate diameter to be used. Once the substrate size is selected (e.g., 50 or 200 mm), the target shape and size and the target-to-substrate spacing, known as throw distance, can be determined. In general, the larger the substrate, the larger the target and the throw distance required. While there are no hard-and-fast rules, a reasonable choice is for the throw distance to be set at least the diameter of the substrate

size if uniform film thickness (±5%) is desired. While some systems allow the throw distance to be varied, such variation is typically not necessary. For most material systems, the same film properties can usually be obtained at different throws by simply changing the background gas pressure, keeping the product of pressure and distance relatively constant. The target diameter should be at least the size of the substrate. Both target and substrate can be mounted in almost any direction; however, there are more advantageous orientations depending on substrate type. Horizontal mounting allows the target (or targets) to be simply held by gravity and the substrate to be suspended at its edges without the need for clamping to a back-plate. Horizontal mounting is important when delicate substrates are used or when the process is sensitive to substrate temperature, or if the quality or integrity of the back side of the substrate is relevant to the application. Regardless of the mounting orientation, if a uniform film thickness is required over substrates larger than 50 mm in diameter, both the substrate and target must be rotated in conjunction with programmable laser beam rastering (discussed below).

The chamber should include ports for substrate manipulation (rotation and translation, if desired); for target rotation (and indexing, if multiple targets are used); for the laser beam entrance; for vacuum pumps and gauging; and for substrate/target transfers (if a hinged door is not used). In addition, the chamber should have several auxiliary ports. These auxiliary ports might include view ports to see the substrate and target during deposition and to see substrate heater components, including current feedthroughs, thermocouples, and water-cooling connections. View ports should use glass that strongly absorbs the laser radiation, or a safety hazard may arise. For excimer lasers, a simple 3-mm-thick Lucite disk placed over a standard low-profile view port is adequate to absorb radiation. In addition to view ports, it is helpful to have a port that controls a substrate shutter and is used for target precleaning prior to deposition. Depending on the ultimate system goals, ports might also be considered for plume diagnostics such as atomic absorption and/or emission; ellipsometry or other spectroscopies; residual gas analysis; and gas processing sources such as atom, ion, or sputter deposition sources, process gas bleed, and vent valve. Port flanges can be knife-edge or O-ring style. It is usually well worth the time to lay out all of the ports on the chamber with each potential component drawn in, prior to fabrication of the chamber. This layout will help ensure that the design can be assembled as intended.

5.7.2.3 Substrate Heater

Careful attention should also be given to substrate heating when designing a PLD tool. Maximum substrate temperatures, along with the type of substrate (as defined by its absorptivity and emissivity) and background gas, are key ingredients in determining the type of heaters to be used. The use of oxygen as a background gas significantly reduces the types of heaters that can be used, especially if the substrate temperature is to reach above ~600°C. Also, if oxygen or other reactive gases are to be used, care must be taken to properly select all the other materials that will become heated in the presence of the gas. Materials such as molybdenum or tungsten should not be used for heating elements, shields, substrate holders, or substrate clips, as they are easily ignited and very dangerous when heated in the presence of oxygen. The design of substrate heaters is considered somewhat of an art and is clearly beyond the scope of this chapter. However, the basic considerations for PLD applications are presented.

One of the first considerations in the design of a substrate heater is whether or not the substrate can be bonded to a heated backing plate with some thermally conductive material such as silver paint or indium. Clamping the substrate to a back plate does not ensure good temperature uniformity and is not recommended for most applications. Although thermal bonding materials (e.g., paint and pastes) provide the easiest way to achieve a given substrate temperature, they have several drawbacks.

- Thermal bonding will be a problem if the back side of the substrate will be used for subsequent film growth (for instance, double-sided YBCO film growth on $LaAlO_3$ substrates), or if the substrates are delicate (such as CdTe or HgCdTe).
- Thermal bonding will be a problem if photolithography will be employed. After deposition, the thermal bonding agent will adhere to the substrate back side and will be difficult or impossible to remove without damaging the deposited film.
- The thermal paste will also outgas a large amount of organic residue during the pumpdown and initial substrate heat cycle.
- If indium is used, it will form an oxide at elevated temperatures. InO has a high vapor pressure and thus will be a possible source of film contamination.
- When bonding large substrates greater than 1 in., it is difficult to ensure uniform bonding after heating up the substrate because the substrate may bow slightly, producing local cold spots.

If bonding is not going to be employed for substrate heating, then more stress is placed on the heating elements to achieve the desired substrate temperature. In this case, however, the substrate back side remains clean, making it easy to either deposit a back-side film or to do postdeposition processing. When not using thermal bonding agents, it is best to hold the substrate only at its edges during the heating process.

Several types of heaters have been used for the PLD process, including projection lamps and resistive heaters based on magnesium oxide (MgO)-sheathed Inconel conductors, nichrome, Kanthal, and platinum. Other combinations of materials have been used for heaters, including Si, SiC, and graphite encapsulated in boron nitride. The latter heating material is very useful for several applications, but if the temperature (not substrate temperature) exceeds ~800°C, the boron nitride is etched by oxygen, if oxygen is used as a process gas. If oxygen is not going to be used, heating elements made from carbon, molybdenum, tantalum, or tungsten wires may be acceptable. When designing a heater, careful consideration must be given to all the materials being used to ensure compatibility with any of the background or process gases and with the ultimate temperature to be reached. Also, care must be taken to make sure that the heating elements or other hot components do not decompose in the desired background gas.

One important figure of merit for any substrate heater is the temperature uniformity attainable across the substrate surface. In order to minimize temperature gradients and the amount of power necessary to heat the substrate to a desired temperature, heating elements should extend out past the edges of the substrate. Several reflecting shields should also be placed above and around the elements and substrate if possible, especially if the substrate temperature is to go beyond ~400°C. These shields will help improve the temperature uniformity and will reduce the amount of power required to heat the substrate to a given temperature. In addition, the shields will reduce the amount of radiation reaching the chamber walls.

Measuring the temperature of a heated substrate can also be difficult, depending on the heater design and substrate materials. For instance, transparent substrates such as sapphire and quartz do not readily absorb IR radiation. Furthermore, when a pyrometer is used to read the temperature of a transparent substrate, the signal from the substrate is obscured by the radiation from whatever is behind the substrate. The result can lead to an incorrect reading. A small thermocouple placed on the substrate itself will not indicate the proper temperature, because the thermocouple will absorb more radiation than the substrate, again indicating the wrong temperature. Thus, measurement of substrate temperature can be very tricky, and care must be taken to obtain the correct value. Sometimes the substrate temperature will not be known, but reproducible growth can be obtained by using a free-floating thermocouple that monitors the radiation environment. The thermocouple should be used as the input to a programmable temperature controller. The temperature

controller can then be used to run predetermined thermal cycles and to hold the temperature constant during deposition.

Another issue when designing a substrate heater is the total amount of energy that will be radiated into the deposition chamber and its effect on other internal components. A properly designed heater for a 3 in. diam substrate needs about 1.5 kW of power to heat a transparent substrate, such as sapphire, to a temperature of 750°C, if no thermal paste is used to bond the substrate to a heated block. The radiation from the heater, if not properly dealt with, can cause several problems. To avoid the problems, properly designed water-cooled plates should be placed behind the heating elements and any of the reflecting shields. This removes excess heat, which otherwise will heat the chamber walls and cause a burn hazard. Furthermore, during processing, hot walls liberate water vapor (usually the dominant source of background gas in any clean and unbaked vacuum system), which can severely influence the properties of the deposited films. A hot substrate (or heater) located a few inches above the target surface can increase the temperature of the target by several hundred degrees. This temperature increase can cause the targets to outgas considerably and may have other, more deleterious effects on film growth. For example, if the target becomes sufficiently hot from the thermal radiation, the absorbed light from the incident laser beam may be sufficient to locally melt the target surface. Local melting greatly increases the ejected particulate density and produces changes in the deposition rate and film properties. Therefore, water-cooled shields should be placed above the target to minimize the thermal radiation, as shown schematically in Figure 5.15. These shields should include slots to expose the necessary area of the target to the laser beam and to allow the plume to impinge on the substrate. Finally, when designing a substrate heater, the following safety issue should be considered: The heater should not be allowed to operate above a few torr. Thus, if the chamber is opened, an operator's hand cannot accidentally touch one of the electrical feedthroughs, causing electric shock.

5.7.2.4 Target

For simple single-layer film growth, only a simple target holder and rotary feedthrough are required. Target rotation is necessary as a minimum; otherwise, the target morphology changes very quickly under laser irradiation, greatly altering the plume shape and direction. Several types of rotary feedthroughs are available for target rotation. Rotation speeds between 6 and 30 rpm are more than adequate for most applications. If the application requires multilayer film growth of different materials, then a multitarget manipulator is required. A manipulator allows the user to readily change, either via computer or manual control, the active (ablation) target without breaking vacuum. Typical manipulator configurations can include from three to six targets of a given size. Figure 5.16 shows a photograph of a multitarget manipulator that holds four 2 in. diam targets. This particular manipulator is mounted on a large 12 in. diam mother flange and has a linear translation stage that provides up to 4 in. of z-axis motion. A programmable stepper motor is supplied, which allows the targets to be quickly indexed into the ablation position in any order desired. This manipulator is based on a dual-axis, magnetically coupled rotary feedthrough. One axis provides continuous target rotation up to 35 rpm; the other axis provides target indexing. The magnetically coupled feedthrough is used because it provides longer life than a welded-bellows feedthrough. The manipulator in Figure 5.16 also has a water-cooled shield that sits directly above the targets. The shield has an open slot to allow rastering of the laser beam over the active target. Note that the shield design protects the unused targets from backscattered vapor, which minimizes cross contamination, and the water-cooling keeps the targets, gears, and bearings isolated from thermal radiation.

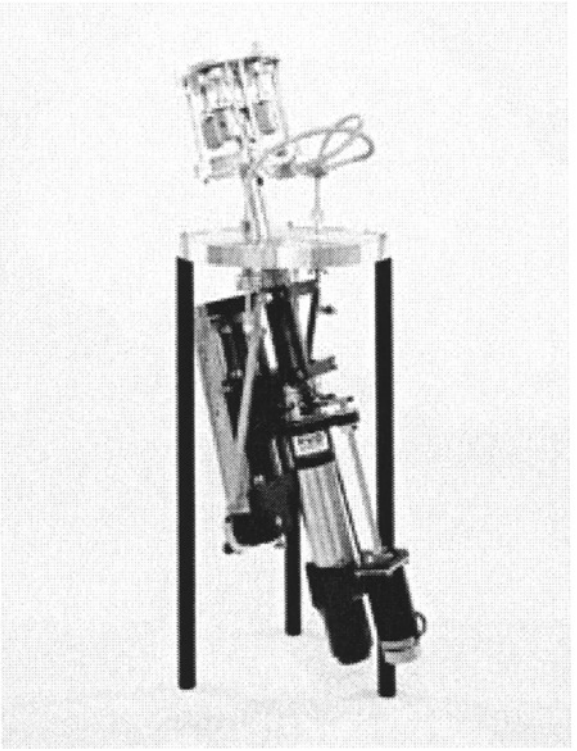

Fig. 5.16. A four-position PLD target manipulator. Photo Courtesy of Epion Corporation.

Almost any material can be deposited by PLD. It is often said that if you can make a solid target of any size and shape, then you can deposit a film by PLD. One interesting example comes to mind. At a Materials Research Society meeting in Boston, a researcher showed an x-ray diffraction θ-2θ scan obtained from a PLD film grown from a small rock taken from the Berlin wall! This example also highlights the fact that the purity of the target is very important. If the element (desired or not) is in the target, it is most likely going to end up in the film. Thus, if the material being deposited is strongly affected by impurities, care should be taken to purchase a target with very high purity. In addition, the targets should be handled with clean gloves.

The target properties (size and density) can play a role in the quality of the films that are produced. Typically, round targets, from one to several inches in diameter, are used. Target thickness can vary from below 0.1 to 0.25 in. or greater. In general, larger diameter targets are more effective than smaller diameter targets, especially if large substrates are to be coated or if very thick films are desired. Larger targets are effective because a large amount of material will be removed from the target. If a large target is used in conjunction with laser beam rastering, the target surface will remain flat, which is preferable. Conversely, if small-diameter targets are used without rastering, the target surface will become trenched as the target is rotated. As a result, the ablation plume angle will be grossly altered, changing the deposition rate at the substrate.[73] Also, the trenching of the target surface will alter the laser beam spot size and thus the laser fluence. Laser rastering using a programmable mirror, discussed in the section below, eliminates trenching of the target surface and provides for more uniform and reproducible deposition.

When obtaining targets for the PLD process, density is also a consideration. It is widely believed that dense targets produce films with the least amount of particulates. This belief is often,

though not always, borne out in reality. Though a dense target is desirable, it is also important that the target be homogeneous with very small grains. However, in order to obtain high density, the target is sintered for a long time, but this also yields larger grain sizes. Therefore, a compromise must be struck between target density and the grain size within the target. A low target density means it is porous but has a small grain size. This porosity will result in outgassing, and for large targets, a considerable amount of pump-out time might be needed before the chamber reaches a base pressure. For some materials, target densities in the 80% range have yielded very good film properties. In other materials, like the carbide targets, vendors will supply either hot-pressed or CVD-prepared targets. The hot-pressed targets tend to generate films with more particulates than CVD-prepared targets. However, CVD carbide targets are very difficult and expensive to obtain. In some cases, powder of the proper material can be ablated. Also, liquid Ga has been used as a target to form GaN films in various background gases. For most materials, the target composition should be exactly the same as the composition desired in the film. However, for certain materials, such as those containing high vapor pressure elements like Pb or Li, nonstoichiometric targets should be considered. The reason is that some of the elements will re-evaporate from the heated substrate surface before being oxidized. In some cases, such as the oxide films, the target can be nonstoichiometric. For instance, MgO and SiO_2 may be formed in an oxygen background using either a simple Mg or SiO target, respectively. Stoichiometric targets would be difficult to obtain directly because of the poor absorption in the UV of these materials.

The morphology of the target surface changes as the ablation process is carried out.[73] For systems that use a fixed-position (nonrastered) laser beam, the target needs to be resurfaced after each run, or after every few runs. Target resurfacing wastes material and raises the issue of contamination of subsequent films.

5.7.2.5 BDS

While the laser has already been discussed, consideration must also be given to the entire BDS that delivers the laser radiation to the ablation target. Two basic approaches to the BDS can be used: focusing and imaging. Usually, fluences between 1 and 3 J/cm^2 are sufficient for most materials, with the actual fluence hitting the target being between 50 and ~500 mJ. Again, because several of the materials of interest to aerospace engineers have high ablation thresholds and low deposition rates, fluences approaching 5 J/cm^2 may be necessary. In general, low fluence and high laser repetition rates are better for producing films than high fluence and low repetition rates. In a simple BDS, the basic elements are an aperture used to define and remove the nonuniform portions of the excimer beam, a focus lens (spherical or cylindrical), and a chamber entrance window. The excimer laser beam is usually 1 × 2 cm in size. Thus, optics of at least 50 mm in diameter should be used. Anti-reflective (AR) coatings are useful for minimizing the laser energy loss at the lens and/or window surfaces. The AR coatings are wavelength specific and will be damaged by radiation at other wavelengths. A more complex BDS can be employed, including multiple focusing lenses, raster mirrors, and beam homogenizers. Laser beam homogenizers are usually not necessary for the PLD process, especially if the laser is operating properly. Raster mirrors are very useful for scanning the laser beam over a large diameter target.[73] Rastering the beam greatly improves the uniformity of film properties such as film thickness and composition. Furthermore, by rastering the laser beam over a large target, the target surface morphology does not significantly change during time. The result is reproducible film growth without the need for resurfacing of the target after each deposition.

Care should be taken to properly deal with reflections that occur at all of the BDS surfaces. These reflections can cause damage to optical components and can become a safety issue. Thus,

it is wise to enclose the BDS in an appropriate box that will absorb the stray radiation. For excimer lasers, a Lucite box is strongly absorbing and quite adequate for the job.

During deposition, the ablated products typically coat the entrance window of the chamber.[74] The amount of the coating depends on several factors, including typical operation pressure, the distance from the target to window, and the angle that the laser makes with the target surface. This coating reduces the laser fluence that is incident on the ablation target. The consequence of this reduction is a change in the deposition rate and the energetics of the ablation process. This change potentially results in nonuniform deposition and in process variability during the film growth. Furthermore, it is well known that changes in fluence affect the as-deposited stress in PLD films. This deleterious effect can be somewhat minimized by the injection of a "curtain" of process gas over the entrance window and by the intelligent choice of the incident angle (e.g., at least 45 deg, or smaller than 30 deg relative to the surface normal) that the laser beam makes with respect to the target surface. Figure 5.17 shows a PLD product, called the Intelligent Window, that not only helps to minimize coating on the window but also provides a direct measure of the energy that actually enters the deposition chamber. For this window, a large transparent disk is housed inside a pair of vacuum flanges. The laser radiation enters the Intelligent Window through a high-quality AR-coated window. The backscattered material is deposited onto the transparent disk over a small area defined by an internal aperture. When this area has become coated with vapor, the disk can be easily rotated, exposing a clean surface via an external feedthrough. A small port is included to bleed the process gas into the area around the disk and aperture, thereby raising the local gas pressure, which also helps keep the disk clean. When the disk becomes fully coated, it can be easily removed and replaced with another disk. The disks can be polished and reused multiple times. Another important feature of the Intelligent Window is that it allows the user to monitor the energy that enters the chamber just prior to deposition of the film. This capability enables the user to achieve reproducible deposition rates and overall film quality. Monitoring the energy is preferable to relying on the laser's energy meter. This meter does not provide a good measure of the energy hitting the target, for a variety of reasons.

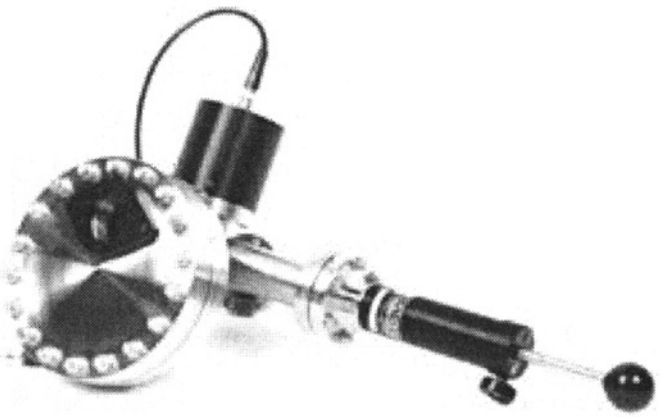

Fig. 5.17. Intelligent Window, which keeps the vacuum chamber window clean for extended periods of time and allows the user to monitor the energy that enters the deposition chamber. Photo courtesy of Epion Corporation.

- The laser beam is multimoded, and the beam divergence depends on factors such as gas fill quality and laser optics. As the beam divergence changes, the energy hitting the target can change considerably (by as much as 25%), depending on other aspects of the overall optical train.
- Quartz optics are well known to produce so-called color centers under intense radiation in the UV. The optics produce a red fluorescence under exposure when a sufficient number of color centers have been produced. When the color centers are activated, the optics absorb a significant amount of the incident energy, significantly reducing what hits the ablation target.
- Losses also occur as the coatings and reflecting surfaces of mirrors and lenses slowly degrade over time because of UV laser exposure.

Thus, the ability to monitor the energy that actually enters the chamber is the only way to know what is really incident on the target. Because many of the film properties depend strongly on laser fluence, the ability to monitor this energy is key to reproducible film growth results.

5.7.2.6 Pump

Several types of vacuum pumps–such as oil diffusion, cryo-, and turbomolecular pumps supported by a rough-pump–are suitable for the PLD process. Ion pumps are not considered suitable unless one is using a load-locked system and is not planning on using any background process gas during the deposition process. Oil diffusion pumps are not the top recommendation because they can be a source of oil contamination in the deposited films. Turbomolecular pumps offer the best option for most PLD applications. Note that these pumps should not be placed on the bottom of the chamber, where they may be seriously damaged by anything that falls. Turbomolecular pumps come in several sizes and varieties, including a molecular drag style. The drag pumps provide very high gas throughput but reduce the overall compression ratio of the pump. A high compression ratio, however, is not needed for the PLD process. The selection of pump size, measured in liters per second, should be based on the chamber size and the required speed for pumpdown to the necessary base pressure. A properly selected pump should achieve an initial pressure below 1×10^{-6} torr within 2 h of pumping and a base pressure in the low to mid 10^{-7} torr range. Because some targets may outgas considerably, there may be a limit to the base pressure that can be obtained. Appropriate pump sizes are between 100 and 1000 l/s, depending on the overall chamber size. At the base pressure, it is likely that the dominant background gas species will be water vapor. If the materials to be deposited are sensitive to water vapor, then alternative pumping approaches need to be considered, or the chamber walls must be baked out to remove water. The latter approach is not particularly convenient, because it is usually takes time, thus limiting the throughput of the PLD tool. An alternative approach is to incorporate, with added cost, a load-lock facility that minimizes the exposure of the main deposition chamber to atmosphere. Adequate consideration should also be given to the selection of a rough-pump. While dry pumps offer oil-free rough pumping, they are expensive and not needed if the turbomolecular pump is handled properly. A standard rotary-vane mechanical rough-pump is more than adequate for the job. However, if oxygen is to be pumped, then consideration must also be given to the pump oil used (e.g., Fomblin oil or the equivalent), because standard hydrocarbon-based oils become highly explosive with sufficient oxygen entrapment. Similar considerations as those just mentioned should be taken into account if ozone or another toxic gas is being pumped using a cryopump.

In the PLD process, vacuum gauging is necessary, not only to measure the base pressure, but also to monitor the pressure of added background gases. Vacuum gauging should include an ion gauge to determine the chamber base pressure, and either a thermocouple, Convectron, or Pirani gauge to monitor the pressure during the initial stages of the pump-down cycle. A capacitance

manometer capable of measuring from about 1×10^{-4} torr to 200 mtorr is recommended for monitoring the pressure during deposition. The manometer should be located so that it actually samples the pressure in close proximity to the substrate. Monitoring the pressure at the chamber wall is usually inadequate, especially if heated substrates are used, because the pressure near the substrate is strongly dependent on the substrate temperature.

During deposition, a background gas is typically used to either thermalize the plume or to improve the stoichiometry of the gas species in the film. For thermalization, an inert gas such as Ar can be used. It is important to control the background gas pressure for several reasons. First, as the background gas pressure is increased, the amount of gas-phase scattering that occurs in the plume also increases. The backscattering of the atomic and molecular species in the plume is considerably higher than the backscattering of the small particulates generated in the plume. For high gas pressures, the atomic species are scattered away from the substrate. This scattering results in films with poor surface morphology. Thus, the deposition process should be run at the lowest pressure that is compatible with obtaining the other properties desired from the material, if film morphology is also important for the application. Second, it is well known that the background gas pressure plays a significant role in the stress in laser-deposited films. At very low pressures, large compressive stresses are usually generated. As the pressure is increased, the magnitude of compressive stress can be reduced. In some cases, tensile stress can be generated, depending on the film and substrate materials.[75] Stress is usually an issue in very thick films, or in films that will be used for protective or tribological coatings.

In order to control the background gas pressure, several alternate approaches can be used instead of the usual method. In the usual method, gas is bled into the vacuum system using either a needle valve or a mass flow control valve. The pressure is then adjusted by either throttling the gate valve or by varying the speed of the turbomolecular pump. In one alternate approach, a secondary valve with a much smaller conductance is used to allow the gas to be bled from the chamber. In another approach for more advanced PLD tools, the capacitance manometer is used in conjunction with a small stepper-motor-controlled bleed valve. The manometer and bleed valve are employed in a closed-loop feedback system to accurately control the pressure during deposition. Usually, it is best to bleed the process gas into the chamber far from the deposition region in order to provide a more static gas environment around the substrate. As mentioned above, the best place to bleed gas into the system is by the laser entrance window, which also helps the window stay clean. Pointing the gas nozzle directly at the substrate is not recommended, because it will produce a dynamic flow environment around the substrate, resulting in nonuniform film properties.

5.7.2.7 Deposition Rate Monitor

For most applications, the film thickness needs to be well defined and reproducible. Thus, the rate of film growth, and the final film thickness, need to be monitored. There are several types of deposition rate monitors that work well for most PVD processes. The most well-known monitor is the quartz crystal microbalance (QCM). At first glance, it may appear that the QCM is ideal for the PLD process. However, this is not the case, for many different reasons. First, if heated substrates are used, the thermal radiation is usually sufficient to cause the QCM to become unstable. Second, the PLD process produces a highly forward-directed plume. In order to achieve any uniformity over reasonable substrate sizes, laser beam rastering is employed, as previously discussed. This rastering produces a dynamic tooling factor problem for the QCM and makes any real thickness measurement difficult to interpret. Third, the PLD process tends to produce films with a high amount of intrinsic stress. Such stress is sufficient to cause the QCM to stop oscillations or to become highly nonlinear. Therefore, instead of the QCM, ellipsometry or optical

transmission techniques may be used to monitor the deposition rate. These techniques are usually difficult to implement as an *in situ* process monitor.

An alternative approach to deposition rate monitoring for the PLD process is that of atomic absorption (AA).[74] An AA monitor is depicted in Fig. 5.15 as items J (a hollow cathode lamp [HCL]), K (HCL collimated radiation), and L (a detector). In this figure, the monochromatic light beam (K) produced by a hollow cathode lamp (L) (J), selected specifically for one of the materials in the target, passes through the chamber, intercepts the ablation plume, and hits the detector (L). The amount of HCL light absorbed by the specific species within the plume is then a measure of the net flux to the substrate surface. Even when the laser is rastered over the target, the HCL beam intercepts the same volume of the ablation plume. With proper integration techniques and careful calibration, this system can be turned into a useful rate monitor. Such systems are currently under development and are expected to be on the market in the near future.

A wide variety of HCLs are available for most materials of interest to the aerospace engineer, except for carbon. However, a variety of tunable lasers are now coming on the market that may replace the HCL for carbon and for other applications. Thus, it would be wise to include ports for AA in any system that is contemplated.

5.7.2.8 Large-Area PLD

Initially, there was a lot of skepticism that PLD could be scaled to substrates much larger than approximately 1 in. This skepticism was held because of the nonuniform and highly directional nature of the PLD plume.[71] Most applications require the various physical, electrical, optical, and tribological properties of the film to be uniform over much larger areas. Indeed, with the proper techniques previously discussed, the PLD *is* readily scalable to large substrates.[73,76] Using large-diameter rotating targets, in conjunction with programmable laser beam rastering with rotating substrates, excellent uniformity can be achieved over substrates up to 8 in. in diameter. Film thickness uniformity of better than ±4% has been achieved for Y_2O_3 films deposited over 200-mm (8 in.) diam substrates.[76] Furthermore, the compositional uniformity obtained over a 150-mm-diam substrate from a YBCO target was ±1.48%, ±0.17%, and ± 0.36% for the Y, Ba, and Cu species, respectively.[76] Uniform electrical properties such as the T_c (critical temperature) and J_c (critical current density) for YBCO over 75-mm-diam $LaAlO_3$ substrates has also been demonstrated.[71] More recent (unpublished) results for the critical temperature of HTS films indicate that *in-situ* YBCO can be deposited with very high quality over 125 mm (5 in.) diam substrate areas with T_c's as high as 89.6 K and with variations of ±0.5 K. It is expected that with proper engineering, PLD can be scaled to much larger sizes, if needed.

PLD is still an emerging technology. At present, applications for PLD-deposited films have not demanded production-style machines. However, several applications for small-scale production PLD are emerging, including the HTS market. Also, complex films deposited over a 1 m length are being seriously considered for a roll-to-roll application. Thus, it is expected that PLD will soon be a standard production deposition technique for a variety of otherwise hard-to-deposit materials.

5.7.3 The PLD System

A properly designed PLD system will offer an engineer or scientist many years of research and development capabilities without the need for major modification or upgrades. Several vendors that offer commercially available systems are listed in Table 5.6. These vendors can also provide components for "in-house" systems. Therefore, the user must decide whether to purchase a complete system or components or whether to assemble the unit in-house. Care should be taken when purchasing a PLD system from a vendor. Vendors who use their own systems to deposit material

Table 5.6. Vendors of PLD Systems

Vendor	Location
DCA Instruments, Inc.	Woburn, Massachusetts
Epion Corporation	Bedford, Massachusetts
Kurt J. Lesker Co.	Clairton, Pennsylvania
Neocera, Inc.	College Park, Maryland
Surface Equipment, Ltd.	Huckelhoven, Germany
Thermionics, Inc.	Hayward, California

on a routine basis are much more likely to deliver a working end-product. While complete systems assembled by vendors may be more expensive, they should provide the user with an operational system in a comparatively short time. Thus, the user will be able to focus on materials development rather than deposition system design.

Figures 5.18 and 5.19 display photographs of a complete PLD system based on a rectangular box design. This load-lock compatible PLD system can handle up to 3 in. diam substrates and can provide very uniform thin films. The system includes a three-position large-diameter target manipulator, an Intelligent Window, a turbomolecular pump, and a rastered optical train. The substrate heater uses IR heat lamps and can heat transparent substrates to temperatures in excess of 800°C in oxygen. In Fig. 5.18, the excimer beam is seen traveling through the optical train on the

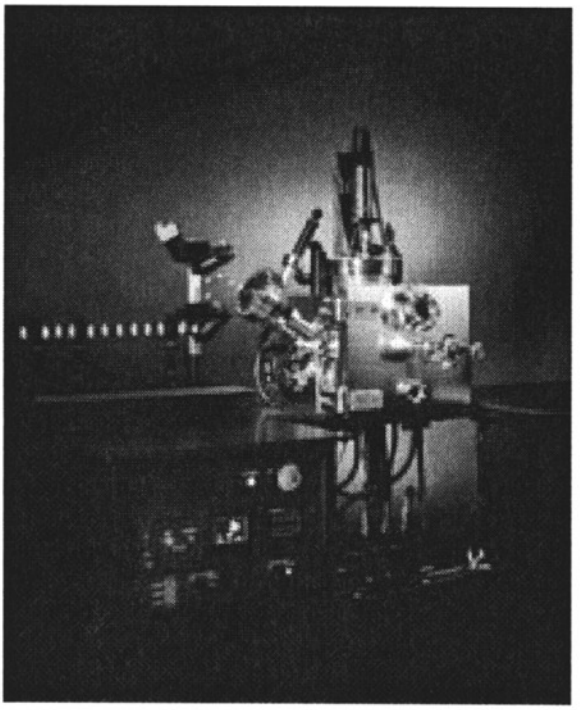

Fig. 5.18. A PLD system for coating 3-in.-diam substrates. Photo courtesy of Epion Corporation.

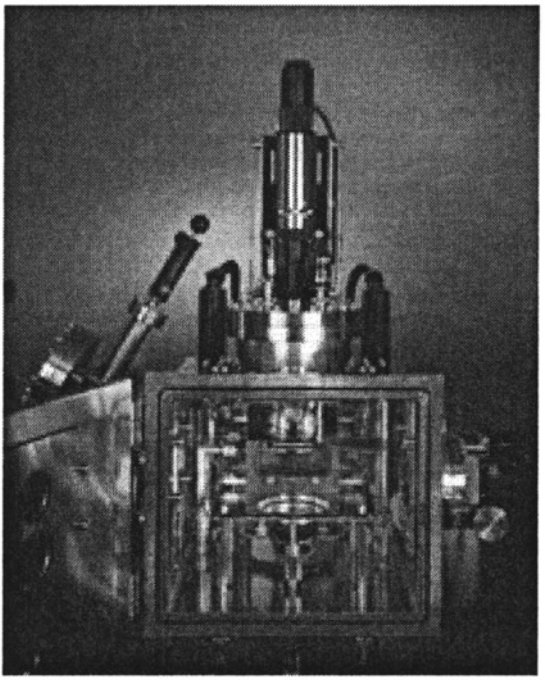

Fig. 5.19. Interior of the PLD system shown in Fig. 5.18 with door ajar. Photo courtesy of Epion Corporation.

left, where it enters the chamber through the Intelligent Window. Also shown in this figure is the linear/rotary feedthrough, on the top of the chamber, for substrate manipulation; the temperature control unit; an emergency off (EMO) button; and the chamber frame and support table. A water manifold is seen below the chamber, which provides several water lines that enter the bottom of the vacuum system. The large door on the chamber can be opened upon venting, as seen in Fig. 5.19, which allows the user to quickly change targets and substrates without removing any of the flange assemblies. Also shown in this figure is the target assembly (below the flat water-cooled plate), the water-cooled heater boxes, the water lines, the shutter, and the substrate rotation stage.

5.8 Conclusions and Brief Overview of Trends

It is clear that laser material processing tools will play a significant role in the future development of new materials and devices. This prediction is made because, by its very nature, laser processing is a "dry," environmentally friendly technique, which under controlled conditions can process materials with minimum waste. We believe that in the near term, laser processing will more likely be applied "at the back end" of a manufacturing process–used for customizing items, enabling precision modifications, and performing repairs. However, the trend for "front-end" laser-processing operations will grow as the cost and reliability of lasers are improved. There are already applications where laser processing in the front end of a manufacturing line is close to being cost effective (e.g., in surface texturing). The Department of Energy's (DOE's) JLAB FEL group is attempting to tip the scales by demonstrating that laser photons can be made for less than 10 cents per kJ of light. Several major U. S. corporations (e.g., Dupont, 3M, IBM, and Northrop Grumman) have formed an industrial consortium (Laser Processing Consortium) in support of this FEL demonstration.

We see laser-based processing techniques especially growing in microengineering applications. We forecast the development of laser tools (e.g., for soldering, phase hardening, sintering) that will enable the manufacturing of microfabricated devices on a desktop[77] to larger laser systems that are designed for volume manufacturing applications (e.g., laser marking, fabrication of masters, selective removal etching, surface texturing).[78] Furthermore, with the desire in the aerospace community to fabricate better or more robust materials (e.g., diamond and SiC for hypersonic vehicles), the use of laser-coating tools like PLD will be more in demand.

The laser vendors and the laser-processing community are also taking steps to provide a better product and more reliable processes. Lasers will continue to get more reliable as they are implemented in manufacturing. A strong technological driver that will increase laser reliability is the decision of the microelectronics industry to use lasers in the lithography of submicron circuits. As a consequence, developers of laser-processing tools are now implementing user-friendly software and additional controls to increase reliability and reduce process variability. In the horizon are other laser sources, currently under development, that will accelerate laser processing. For example, single-mode fiber lasers have achieved power levels approaching 1 W, and one can conceive of bundling many fibers together for higher power. Furthermore, there continues to be an increase in the power of diode-pumped solid-state lasers. These systems are approaching kilowatt power levels, and their total footprint in size is diminishing. Also expected in the market are femtosecond lasers and vacuum UV (VUV) (157-nm) excimer-laser-based material processing tools.

Finally, in the aerospace community, and especially for space applications, there is a growing trend to design systems, and for that matter, satellites, as complete integrated packaged units.[79] To implement this concept, the aerospace community will need to borrow heavily from the microelectronics industry. This means more automation in the manufacturing segment, use of clean processes, more use of CADCAM software, reliability assessments based on statistical measurements, and the general miniaturization and integration of common systems. Laser-based tools are poised to make significant impact to this development.

5.9 References

1. R. S. Muller, R. T. Howe, S. D. Senturia, R. L. Smith, and R. M. White, *Microsensors* (IEEE Press, NY, 1991); J. Bryzek, "MEMS: A Closer Look," *Sensors*, 5 (July 1996); *Microengineering Technology for Space Systems*, Monograph 97-02, edited by H. Helvajian (The Aerospace Press, Los Angeles, 1997).
2. H. Helvajian, "Laser Material Processing: A Multifunctional in-situ Processing Tool for Microinstrument Development," in *Microengineering Technology for Space Systems*, Monograph 97-02, edited by H. Helvajian (The Aerospace Press, Los Angeles, 1997), p. 67 and references therein.
3. R. E. Russo, D. B. Geohegan, R. F. Haglund, Jr., and K Murakami, editors, *Laser Ablation* (Elsevier, New York, 1997); J. F. Ready, *Effects of High-Power Laser Radiation* (Academic Press, NY, 1971); J. Y. Tsao and D. J. Ehrlich, editors, *Laser Microfabrication –Thin Film Processes and Lithography* (Academic Press, NY, 1989); R. Haglund, Jr., and R. Kelly, "Electronic Processes in Sputtering by Laser Beams," in *Fundamental Processes in Sputtering of Atoms and Molecules*, edited by P. Sigmund (Munksgaard, Copenhagen, 1993); L. D. Laude, D. Bäuerle, and M. Wautelet, editors, *Interfaces Under Laser Irradiation*, NATO ASI series E-134 (Martinus, Nijhoff Publishers, Boston, 1987); Y-K Swee, H-Y Zheng, and R. T. Chen, *Microelectronic Packaging and Laser Processing* (SPIE Publications, Washington, 1997); W. M. Steen, *Laser Material Processing* (Springer, NY, 1998); H. E. Pontath and G. I Stegeman, editors, *Nonlinear Surface Electromagnetic Phenomena, Modern Problems in Condensed Matter Physics* (North Holland Press, NY, 1991), Vol. 29; R. M. Osgood, Jr., editor, *Laser-Assisted Microtechnology*, Springer Series in Materials Science, (Springer, NY, 1998), Vol. 19.
4. W. W. Duley, *Laser Processing and Analysis of Materials* (Plenum Press, NY, 1983), p. 37.

5. An-S. Chu, S. H. Zaidi, and S. R. J. Brueck, "Fabrication and Raman Scattering Studies of One-Dimensional Nanometer Structures in (110) Silicon," *Appl Phys. Lett.* 63 (7), 905 (1993).
6. Y. Lu *et al.*, "Wet-Chemical Etching of Mn-Zn Ferrite by Focused Ar^{+}-Laser Irradiation in H_3PO_4," *Appl. Phys.* A47, 319 (1988).
7. M. Rothschild and D. Ehrlich, "A Review of Excimer Laser Projection Lithography," *J. Vac. Sci. Technol.* B6, 1 (1988).
8. H. Kumagai *et al.*, "Ablation of Polymer Films by a Femtosecond High Peak Power Ti:Sapphire Laser at 798 nm," *Appl. Phys. Lett.* 65, 1850 (1994).
9. J. Ouellette, "Free-Electron Lasers: A Radical Alternative," *Indust. Phys.* 3, 18 (1997).
10. S. Silverman, R. Aucoin, J. Mallatt, and D. Ehrlich, "Laser Microchemical Technology: New Tools for Microsystems Engineering, Debug and Failure Analysis," *SPIE* 2991, 129–137 (1997).
11. J. H. Brannon, J. R. Lankard, A. I. Baise, F. Burns, and J. Kaufman, "Excimer Laser Etching of Polyimide," *J. Appl. Phys.* 58, 2036–2043 (1985).
12. W. W. Hansen, S. W. Janson, and H. Helvajian, "Direct-Write UV Laser Microfabrication of 3D Structures in Lithium-alumosilicate Glass," *SPIE* 2991, 104–112 (1997).
13. N. Nassuphis, R. H. Mathews, S. T. Palmacci, and D. J. Ehrlich, "Three Dimensional Laser Direct Writing: Applications to Multichip Modules," *J. Vac. Sci. Technol. B.* 12(6), 3294–3295 (1994).
14. G. M. Daly, D. B. Chrisey, J. M. Pond, M. Osofsky, M. Miller, P. Lubitz, J. S. Horwitz, R. C.Y. Auyeung, and R. J. Soulen, Jr., "Pulsed Laser Deposition of High Temperature Superconducting and Metallic Thin Films for Novel Three Terminal Device Applications," *SPIE* 2991, 226–237 (1997).
15. V. I. Konov, F. Dausinger, S. V. Garnov, S. M. Klimentov, T. V. Kononenko, and O. G. Tzarkova, "Ablation of Ceramics by UV, Visible and IR Pulsed Laser Radiation," *SPIE* 2991, 151–160 (1997).
16. F. Gonella, G. Mattei, P. Mazzoldi, E. Cattaruzza, G. W. Arnold, G. Barraglin, P. Calvelli, R. Polloni, R. Bertoncello, and R. F. Haglund, Jr., "Interaction of High-Power Light with Silver Nanocluster Composite Glasses," *Appl. Phys. Lett.* 69, 3101–3103 (1996).
17. M. Rothschild, C. Arnone, and D. J. Ehrlich, "Excimer-Laser Etching of Diamond and Hard Carbon Films by Direct-Writing and Optical Projection," *J. Vac. Sci. Technol. B.* 4, 310–314 (1986).
18. I. W. Boyd, "Doping and Oxidation," in *Laser Microfabrication–Thin Film Processes and Lithography*, edited by J. Y. Tsao and D. J. Ehrlich (Academic Press, NY, 1989), p. 542.
19. S. H. Zaidi and S. R. J. Brueck, "Multiple-Exposure Interferometric Lithography," *J. Vac. Sci. Technol. B.* 11(3), 658 (1993).
20. A. G. Cullis, H. C. Webber, and P. Bailey, "A Device for Laser Beam Diffusion and Homogenization," *J. Phys. E. Sci. Instrum.* 12, 688 (1979).
21. H. Kogelnik, and T. Li, "Laser Beams and Resonators," *Proc. IEEE 54* (1966), p. 1312.
22. A. E. Siegman, *Lasers* (University Science Books, Mill Valley CA, 1986), p. 676.
23. M. Born and E. Wolf, *Principals of Optics*, 5th ed. (Pergamon Press, NY, 1975) p. 419.
24. D. J. Ehrlich, J. Y. Tsao, C. O. Bozler, "Submicron Patterning by Projected Excimer Laser-Based Beam Induced Chemistry," *J. Vac. Sci. Technol. B3*, 1 (1985).
25. Y. S. Liu, "Sources, Optics and Laser Microfabrication Systems for Direct Write and Projection Lithography," in *Laser Microfabrication--Thin Film Processes and Lithography*, edited by J. Y. Tsao and D. J. Ehrlich (Academic Press, 1989), p. 3.
26. K. M. A. El-Kader, J. Oswald, J. Kocka, and V. Chab, "Formation of Luminescent Silicon by Laser Annealing of a-Si:H," *Appl. Phys. Lett.* 64, 2555 (1994).
27. G. V. Treyz, R. Beach, and R. N. Osgood, Jr., "Rapid Direct Writing of High Aspect-Ratio Trenches in Silicon," *Appl. Phys. Lett.* 50, 475 (1987).
28. G. B. Shinn, F. Steigerwald, H. Stiegler, R. Sauerbrey, F. K. Tittle, and W. L. Wilson Jr., "Excimer Laser Photoablation of Silicon," *J. Vac. Sci. Technol. B4*, 1273 (1986).
29. M. Ishii, T. Meguro, T. Sugano, K. Gamo, and Y. Aoyagi, "Digital Etching by Using a Laser Beam: On the Control of Digital Etching Products," *Appl. Surf. Sci.* 79/80, 104 (1994).
30. J. Y. Tsao and D. J. Ehrlich, editors, *Laser Microfabrication –Thin Film Processes and Lithography*, edited by (Academic Press, NY, 1989); R. Haglund, Jr., and R. Kelly, "Electronic Processes in Sput-

tering by Laser Beams," in *Fundamental Processes in Sputtering of Atoms and Molecules*, edited by P. Sigmund (Munksgaard, Copenhagen, 1993).
31. M. Eyett and D. Bauerle, "Influence of the Beam Spot Size on Ablation Rates in Pulsed-Laser Processing," *Appl. Phys. Lett.* 51, 2054 (1987).
32. C. I. H. Ashby, "Laser Driven Etching" in *Thin Film Processes II* (Academic Press, NY, 1991), p. 783.
33. D. V. Podlesnik, H. H. Gilgen, and R. M. Osgood, Jr., "Waveguiding Effects in Laser-Induced Aqueous Etching of Semiconductors," *Appl. Phys. Lett.* 48, 496 (1986).
34. R. J. Wallace, M. Bass, S. M. Copley, "Curvature of Laser-Machined Grooves in Si3N4," *J. Appl. Phys.* 59, 3555 (1986).
35. C. Kittel, *Introduction to Solid State Physics*, 6th ed. (John Wiley & Sons, NY, 1986).
36. D. Ashkenasi, A. Rosenfeld, H. Varel, M. Wahmer, and E. E. B. Campbell, "Laser Processing of Sapphire with Picosecond and Sub-picosecond Pulses," *Appl. Surf. Sci.* 120, 65 (1997).
37. L. Wiedeman and H. Helvajian, "Laser Photodecomposition of Sintered YBCO: Ejected Species Population Distributions and Initial Kinetic Energies for the Laser Ablation Wavelengths 351, 248, and 193," *J. Appl. Phys.* 70, 4513 (1991); H. Helvajian and R. Welle, "Threshold Level Laser Photoablation of Crystalline Silver: Ejected Ion Translational Energy Distributions, *J. Chem. Phys.* 91, 2616 (1989); H. Helvajian, "Surface Excitation Mediated Physics in Low-Fluence Laser Material Processing," *SPIE* 2403 1 (1995); R. H. Ritchie, J. R. Manson, and P. M. Echenique, "Surface Plasmon-Ion Interaction in Laser Ablation of Ions from a Surface," *Phys. Rev. B.* 49, 2963 (1994); D. P. Taylor, W. C. Simpson, K. Knutsen, M. A. Henderson, and T. M Orlando, "Photon Stimulated Desorption of Cations from Yttria-Stabilized Cubic ZrO_2(100)," in *Laser Ablation*, edited by R. E. Russo, D. B. Geohegan, R. F. Haglund, Jr., and K Murakami (Elsevier, NY, 1997), p. 101.
38. J. F. Ready, *Effects of High-Power Laser Irradiation* (Academic Press, NY, 1971).
39. C. I. H. Ashby, J. Y. Tsao, "Photophysics and Thermophysics of Absorption and Energy Transport in Solids" in *Laser Microfabrication--Thin Film Processes and Lithography*, edited by J. Y. Tsao and D. J. Ehrlich (Academic Press, NY, 1989), p. 272.
40. J. T. Dickinson, S. C. Langford, J. J. Shin, and D. L. Doering, "Positive Ion Emission from Excimer Laser Excited MgO Surfaces," *Phys. Rev. Lett.* 73, 2630 (1994).
41. F. Wood, and D. H. Lowndes, "Laser Processing of Wide Band Gap Semiconductors and Insulators," *Cryst. Latt. Def. and Amorph. Mat.* 12, 475 (1986); A. H. Guenther, and J. K. Mciver, "The Role of Thermal Conductivity in the Pulsed Laser Damage Sensitivity of Optical Thin Films," *Thin Solid Films* 163, 203 (1988).
42. L. P. Welsh, J. A. Tuchman, and I. P. Herman, "The Importance of Thermal Stresses and Strains Induced in Laser Processing with Focused Gaussian Beams," *J. Appl. Phys.* 64, 6274 (1988).
43. A. L. Dawar, S. Roy, T. Nath, S. Tyagi, and P. C. Mathur, "Effect of Laser Annealing on Electrical and Optical Properties of n-Mercury Cadmium Telluride," *J. Appl. Phys.* 69, 3849 (1991).
44. M. Raff, M. Schutze, C. Trappe, R. Hannot, and H. Kurz, "Laser-Stimulated Nonthermal Particle Emission from InP and GaAs Surfaces," *Phys. Rev. B* 50, 11031 (1994);
45. H. Helvajian and R. Welle, "Threshold Level Laser Photoablation of Crystalline Silver: Ejected Ion Translational Energy Distributions," *J. Chem. Phys.* 91, 2616 (1989).
46. L. P. Smith, "The Emission of Positive Ions from Tungsten and Molybdenum," *Phys. Rev.* 35, 381 (1930).
47. A. N. Pirri, R. G. Root, P. K. S. Wu, "Plasma Energy Transfer to Metal Surfaces Irradiated by Pulsed. . .," AIAA J. 16, 1296 (1978).
48. L. Spitzer, *Physics of Fully Ionized Gases* (Wiley-Interscience, NY, 1956).
49. A. C. Tam, *et al.*, "Experimental and Theoretical Studies of Bump Formation During Laser Texturing of NiP Disk Substrates," *IEEE Trans. Mag.* 32, 3771 (1996).
50. S. Lugomer, *Laser Technology: Laser Driven Processes* (Prentice Hall, Englewood Cliffs, 1990), Chap. 5.

51. L. F. Thompson, "Microlithography: The Physics," in *Introduction to Microlithography*, edited by L. F. Thompson, C. G. Willson, and M. J. Bowden (American Chemical Society, Washington, D.C., 1983), Chap. 1.
52. J. Brannon, *Excimer Laser Ablation and Etching*, AVS Monograph M-10 (American Vacuum Society, NY, 1993), Chap. 6.
53. E. Hecht and A Zajac, *Optics* (Addison-Wesley, Reading, 1974), Chap. 10.
54. A. Marchant, *Optical Recording* (Addison-Wesley, Reading, 1990), Chap. 7.
55. J. Brannon, "Micropatterning of Surfaces by Excimer Laser Projection," *J. Vac. Sci. Technol.* B7, 1064 (1989).
56. Y.S. Liu "Sources, Optics, and Laser Microfabrication Systems for Direct Writing and Projection Lithography," in *Laser Microfabrication: Thin Film Processes and Lithography*, edited by D. J. Ehrlich and J. Y. Tsao (Academic Press, NY, 1989), p. 3; J. J. Ritsko "Laser Etching" in *Laser Microfabrication: Thin Film Processes and Lithography*, edited by D. J. Ehrlich and J. Y. Tsao (Academic Press, NY, 1989), p. 33.
57. A. Berezhnoi, *Glass Ceramics and Photo-Sitalls* (Plenum Press, NY, 1970).
58. *IBM J. Res. Dev.* 36(5) (1992). The September issue is fully devoted to the ES9000 semiconductor and packaging technologies.
59. R. Srinivasan and V. Mayne-Banton, "Self-Developing Photoetching of Poly(ethylene terephthalate) Films by Far-Ultraviolet Excimer Laser Radiation," *Appl. Phys. Lett.* 41, 576 (1982).
60. J. Andrew *et al.*, "Direct Etching of Polymeric Materials Using a XeCl Laser," *Appl. Phys. Lett.* 43, 717 (1983).
61. J. Lankard and G. Wolbold, "Excimer Laser Ablation of Polyimide in a Manufacturing Facility," *Appl. Phys.* A54, 355 (1992).
62. K. Prasad and E. Perfecto, "Multilevel Thin Film Packaging: Applications and Processes for High Performance Systems," *IEEE Trans. Comp. Hybrid Mfg. Tech.* 17, 38 (1994).
63. G. Wolbold, C. Tessler, and D Tudryn, "Polymer Ablation with a High-Power Excimer Laser Tool," *Microelec. Eng.* 20, 3 (1993); J. Lankard and G. Wolbold, "Excimer Laser Ablation of Polyimide in a Manufacturing Facility," *Appl. Phys.* A54, 355 (1992); R. Patel *et al.*, "Laser Via Ablation Technology for MCM-D Fabrication at IBM Microelectronics," *Int. J. Microcircuit Elec. Pack.* 18, 266 (1995).
64. R. Patel *et al.*, "Laser Via Ablation Technology for MCM-D Fabrication at IBM Microelectronics," *Int. J. Microcircuit Elec. Pack.* 18, 266 (1995).
65. W. F. Iceland, "Design and Development of Equipment for Laser Wire Stripping," *SPIE* 86, 68 (1976); J. P. Wheeler, "Industrial Applications of Low-Power CO_2 Lasers," *SPIE* 668, 236 (1986); R. T. Miller, "Laser Wire Stripping," *SPIE* 744, 94 (1987).
66. J. Brannon, A. C. Tam, and R. Kurth, "Pulsed Laser Stripping of Polyurethane-Coated Wires: A Comparison of KrF and CO_2 Lasers," *J. Appl. Phys.* 70, 3881 (1991).
67. K. Ashar, *Magnetic Disk Drive Technology* (IEEE Press, NY 1997), Chap. 1.
68. P. Baumgart, D. Krajnovich, T. Nguyen, and A. C. Tam, "A New Laser Texturing Technique for High Performance Magnetic Disk Drives," *IEEE Trans. Mag.* 31, 2946 (1995).
69. P. Baumgart, D. Krajnovich, T. Nguyen, and A. C. Tam, "Safe Landings: Laser Texturing of High-Density Magnetic Disks," *Data Storage* (March 1996).
70. A. C. Tam, J. Brannon, P. Baumgart, and I. Pour, "Laser Texturing of Glass Disk Substrates," *IEEE Trans. Mag.* 33 (1997).
71. D. B. Chrisey and G. K. Hubler, editors, *Pulsed Laser Deposition of Thin Films* (John Wiley & Sons, Inc., NY, 1994).
72. A.A. Puretzky, C. B. Geohegan, G.E. Jellison, Jr., and M. M. McGibbon, "Amorphous Diamond-Like Carbon Films Growth By KrF- and ArF- Excimer Laser PLD:Correlation with Plume Properties," *MRS* (1995); D. L. Pappas, K.L. Saenger, J. Bruley, W. Krakov, J.J. Cuomo, and R. W. Collins, *J. Appl. Phys.* 71, 5675 (1992).

73. J. A. Greer and M. D. Tabat, "Large-Area Pulsed Laser Deposition: Techniques and Applications," *J. Vac. Sci. Technol. A* 13(3), 1175–1181 (1995).
74. J. A. Greer, M. D. Tabat, and C. Lu, "Future Trends for Large-Area Pulsed Laser Deposition," *Nuclear Instruments and Methods in Physics Research*, B(121), 357–362 (1997).
75. J. A. Greer and M. D. Tabat, "Properties of Laser-Deposited Yttria Films on CdTe and Silicon Substrates," *Mat. Res. Soc. Symp. Proc.* 341, 87–94 (1994).
76. J. A. Greer and M. D. Tabat, "On- and Off-Axis Large-Area Pulsed Laser Deposition," *Mat. Res. Soc. Symp. Proc.* 388, 151–161 (1995).
77. C. Roychoudhuri, "Desk-Top Manufacturing Using Diode Lasers," *SPIE* 3274, 162–170 (1998).
78. G. Ogura and B. Gu, "Review of Laser Micromachining in Contract Manufacturing," *SPIE* 3274, 171–182 (1998).
79. S. Janson, "Spacecraft as an Assembly of ASIMS," in *Microengineering Technology for Space Systems*, Monograph 97-02, edited by H. Helvajian (The Aerospace Press, El Segundo, CA, 1997), p. 143. First published as The Aerospace Corp. Report no. ATR-95(8168)-2 (1995).